CHEMISTRY OF MATERIALS
Article

Chem. Mater. **2010,** *22,* 3961–3982 3961
DOI:10.1021/cm1008703

Tuning Topochemical Polymerization of Diacetylenes: A Joint Synthetic, Structural, Photophysical, and Theoretical Study of a Series of Analogues of a Known Reactive Monomer, 1,6-Bis(diphenylamino)-2,4-hexadiyne (THD)

Jérôme Deschamps,[†] Mirela Balog,[†] Bruno Boury,[†] Mouna Ben Yahia,[‡] Jean-Sébastien Filhol,[‡] Arie van der Lee,[§] Antoine Al Choueiry,[#] Thierry Barisien,[#] Laurent Legrand,[#] Michel Schott,[#] and Sylvain G. Dutremez*,[†]

[†]*Institut Charles Gerhardt Montpellier, UMR 5253 CNRS-UM2-ENSCM-UM1, Equipe CMOS, Université Montpellier II, Bât. 17, CC 1701, Place Eugène Bataillon, 34095 Montpellier Cedex 5, France,* [‡]*Institut Charles Gerhardt Montpellier, UMR 5253 CNRS-UM2-ENSCM-UM1, Equipe CTMM, Université Montpellier II, Bât. 15, CC 1501, Place Eugène Bataillon, 34095 Montpellier Cedex 5, France,* [§]*Institut Européen des Membranes, CNRS-UMR 5635, Université Montpellier II, Case Courrier 047, Place Eugène Bataillon, 34095 Montpellier Cedex 5, France, and* [#]*Institut des NanoSciences de Paris, UMR 75 88 CNRS, Université Pierre et Marie Curie-Paris 6, Campus Boucicaut, 140, rue de Lourmel, 75015 Paris, France*

Received March 26, 2010. Revised Manuscript Received May 17, 2010

Several analogues of 1,6-bis(diphenylamino)-2,4-hexadiyne (THD) have been prepared and their thermal and photochemical solid-state polymerization reactivity assessed. The compounds involved in this investigation are 1,6-bis(dibenzylamino)-2,4-hexadiyne (**1**), 1,6-bis(di-*p*-tolylamino)-2,4-hexadiyne (**2**), 1,6-bis(dipentafluorophenylamino)-2,4-hexadiyne (**3**), 1,6-bis((*N*-pentafluorophenyl)phenylamino)-2,4-hexadiyne (**4**), 1,12-bis(diphenylamino)-5,7-dodecadiyne (**5**), and 1,10-bis(diphenylamino)-4,6-decadiyne (**6**). Compound **6** is the only diacetylene that showed measurable polymerization reactivity, and this behavior was rationalized on the basis of X-ray crystallographic results. Yet, diyne **6** is much less reactive than THD, so the preparation of weakly polymerized single crystals of **6** proved to be possible and the study of the spectroscopic properties of "diluted" poly-**6** chains feasible. Unlike poly-THD, poly-**6** is quite soluble in organic solvents such as chloroform and THF, so determination by SEC of the molecular weight of this polydiacetylene (PDA) could be achieved, M_n = 150 000−300 000 Da. The polymeric chains generated by γ-ray irradiation of single crystals of **6** are highly luminescent, which lends strong support to poly-**6** being a red phase PDA similarly to poly-THD. The transition energy of the exciton for poly-**6**, about 2.4 eV, is much higher than that of poly-THD, 2.171 eV at 16 K. This difference was rationalized on the basis of dissimilarities in the $C_1{=}C_4\cdots C_1{=}C_4$ dihedral angle between the two polymers. The structure of poly-**6** in its monomer matrix was obtained by DFT calculations and, based on this structure, the $C_1{=}C_4\cdots C_1{=}C_4$ dihedral angle of the PDA chain found to be 140°. The $C_1{=}C_4\cdots C_1{=}C_4$ dihedral angle in poly-THD, based on the known X-ray crystal structure of this polymer, is 167°. Thus, poly-**6** appears to be a new structural type of PDAs; it is also a good model for the study of the relationship that exists between chain conformation and electronic structure.

Introduction

Polydiacetylenes (PDAs) are conjugated polymers (CPs) with the general formula $(=CR-C\equiv C-CR'=)_n$ where R and R′ are two of many possible molecular groups that may or may not be different. PDAs are the only CPs that can be obtained in a highly ordered state, either as macroscopic polymer crystals,[1−5] or as perfectly regular isolated chains in their monomer crystal matrix.[6] In this respect, PDAs are the best known approximation to a theoretician's view of a CP, and therefore, they are useful models for studying electronic properties of CPs in the absence (or near absence) of disorder. This situation contrasts with what is observed for all of the other CPs, which are usually amorphous or semicrystalline.

*Corresponding author. E-mail: dutremez@univ-montp2.fr.

(1) Wegner, G. *Z. Naturforsch., B* **1969**, *24*, 824–832.
(2) (a) Baughman, R. H. *J. Polym. Sci., Polym. Phys. Ed.* **1974**, *12*, 1511–1535. (b) Wegner, G. *Pure Appl. Chem.* **1977**, *49*, 443–454. (c) Baughman, R. H.; Chance, R. R. *Ann. N.Y. Acad. Sci.* **1978**, *313*, 705–725. (d) Baughman, R. H.; Yee, K. C. *J. Polym. Sci., Macromol. Rev.* **1978**, *13*, 219–239. (e) Bloor, D. In *Developments in Crystalline Polymers-1*; Bassett, D. C., Ed.; Applied Science Publishers: London, 1982; Chapter 4, pp 151−193. (f) Bloor, D. *Mol. Cryst. Liq. Cryst.* **1983**, *93*, 183–199. (g) Bloor, D. In *Quantum Chemistry of Polymers−Solid State Aspects*; Ladik, J., André, J. M., Seel, M., Eds.; NATO ASI Series C: Mathematical and Physical Sciences; D. Reidel Publishing Co.: Dordrecht, The Netherlands, 1984; Vol. *123*, pp 191−220.
(3) Enkelmann, V. *Adv. Polym. Sci.* **1984**, *63*, 91–136.
(4) *Polydiacetylenes: Synthesis, Structure, and Electronic Properties*; Bloor, D., Chance, R. R., Eds.; NATO ASI Series E: Applied Sciences; Martinus Nijhoff Publishers: Dordrecht, The Netherlands, 1985; Vol. *102*.
(5) Misin, V. M.; Cherkashin, M. I. *Russ. Chem. Rev.* **1985**, *54*, 562–593.
(6) Schott, M. In *Photophysics of Molecular Materials: From Single Molecules to Single Crystals*; Lanzani, G., Ed.; Wiley-VCH: Weinheim, 2006; pp 49−151.

Published on Web 06/11/2010

Scheme 1. Schematic Representation of the Topochemical Principle for Diacetylene Polymerization

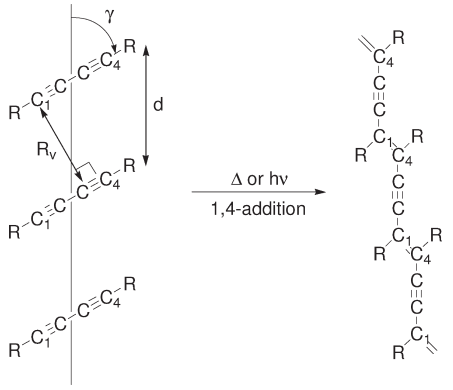

The high order in PDA samples is due to their peculiar (in fact, almost unique) polymerization process. Polymerization proceeds in the solid crystalline state and is a topochemical reaction,[7,8] meaning that all of the reaction steps (initiation by formation of a dimer radical or radical ion, and propagation) are under control of the reactive site geometry and, more generally, of the overall monomer crystal packing. In fact, the limiting step is usually initiation, which is sketched in Scheme 1.[9]

Necessary (but not sufficient) conditions for the topochemical initiation reaction to occur were identified early on: (i) the translational period d of the monomer (see Scheme 1) must be in the range of 4.7 to 5.2 Å; (ii) R_v must be smaller than 4 Å, with a lower limit of 3.4 Å corresponding to van der Waals contact between reacting carbon atoms; (iii) the angle γ between the diacetylene (DA) rod and the translational vector must be close to 45°. All three geometrical requirements should be met in order to secure a close contact between the C_1 atom of one DA rod and the C_4 atom of the neighboring rod, in the reactive monomer crystal.[2,3] These conditions can be fulfilled by a judicious choice of the DA side groups, noting that these groups contain most of the atoms in the molecule and play a leading role in the monomer crystal packing. Therefore, crystal engineering starting from a known reactive DA can lead to new PDAs with new properties.

Another consequence of the topochemical character of the polymerization reaction is that PDA chains contain essentially no defect: a chemical impurity or a geometrical mismatch due to a physical defect do not meet the geometrical requirements, so the propagation reaction stops without incorporation of the defect in the chain. The quasi-perfect character of PDA chains is a consequence of this peculiarity.

In quasi-1D systems, geometrical changes have a very large influence on electronic properties. This is manifested in PDAs by the existence of several ≪colors≫: all of the PDA chains have the same chemical structure, yet their very strong absorption appears in different regions of the visible spectrum. The most frequent colors are traditionally named ≪blue≫ and ≪red≫, with absorption maxima at room temperature around 620 and 540 nm, respectively. The same PDA (that is, with the same side groups) can be found in both colors with a first order transition between them.[10−16] However, the geometrical changes that must necessarily correspond to the large absorption shifts are small, in fact, small enough in some cases to have passed unnoticed in structural studies.[17] Moreover, the different colors have very different emission properties, blue PDAs being virtually nonluminescent and red ones showing a strong emission, at least at low temperature.[18]

Synthesizing and studying PDAs with different colors is a worthy undertaking for two main reasons: (i) fundamentally, it is important to understand how geometrical changes affect the electronic properties of CPs, in particular the consequences of electronic correlations; (ii) in

(7) Hirshfield, F. L.; Schmidt, G. M. J. *J. Polym. Sci., Part A* **1964**, *2*, 2181–2190.
(8) Kaiser, J.; Wegner, G.; Fischer, E. W. *Isr. J. Chem.* **1972**, *10*, 157–171.
(9) Sixl, H. *Adv. Polym. Sci.* **1984**, *63*, 49–90.
(10) Chance, R. R.; Baughman, R. H.; Müller, H.; Eckhardt, C. J. *J. Chem. Phys.* **1977**, *67*, 3616–3618.
(11) Eckhardt, H.; Eckhardt, C. J.; Yee, K. C. *J. Chem. Phys.* **1979**, *70*, 5498–5502.
(12) Koshihara, S.; Tokura, Y.; Takeda, K.; Koda, T.; Kobayashi, A. *J. Chem. Phys.* **1990**, *92*, 7581–7588.
(13) Hankin, S. H. W.; Downey, M. J.; Sandman, D. J. *Polymer* **1992**, *33*, 5098–5101.
(14) Lio, A.; Reichert, A.; Ahn, D. J.; Nagy, J. O.; Salmeron, M.; Charych, D. H. *Langmuir* **1997**, *13*, 6524–6532.
(15) Carpick, R. W.; Mayer, T. M.; Sasaki, D. Y.; Burns, A. R. *Langmuir* **2000**, *16*, 4639–4647.
(16) Lee, D.-C.; Sahoo, S. K.; Cholli, A. L.; Sandman, D. J. *Macromolecules* **2002**, *35*, 4347–4355.
(17) Schott, M. *J. Phys. Chem. B* **2006**, *110*, 15864–15868.
(18) Lécuiller, R.; Berréhar, J.; Lapersonne-Meyer, C.; Schott, M.; Ganière, J.-D. *Chem. Phys. Lett.* **1999**, *314*, 255–260.
(19) (a) Müller, H.; Eckhardt, C. J. *Mol. Cryst. Liq. Cryst.* **1978**, *45*, 313–318. (b) Nallicheri, R. A.; Rubner, M. F. *Macromolecules* **1991**, *24*, 517–525. (c) Carpick, R. W.; Sasaki, D. Y.; Burns, A. R. *Langmuir* **2000**, *16*, 1270–1278.
(20) (a) Tieke, B.; Lieser, G.; Wegner, G. *J. Polym. Sci., Polym. Chem. Ed.* **1979**, *17*, 1631–1644. (b) Okada, S.; Peng, S.; Spevak, W.; Charych, D. *Acc. Chem. Res.* **1998**, *31*, 229–239. (c) Lu, Y.; Yang, Y.; Sellinger, A.; Lu, M.; Huang, J.; Fan, H.; Haddad, R.; Lopez, G.; Burns, A. R.; Sasaki, D. Y.; Shelnutt, J.; Brinker, C. J. *Nature* **2001**, *410*, 913–917. (d) Yuan, Z.; Lee, C.-W.; Lee, S.-H. *Angew. Chem., Int. Ed.* **2004**, *43*, 4197–4200. (e) Peng, H.; Tang, J.; Pang, J.; Chen, D.; Yang, L.; Ashbaugh, H. S.; Brinker, C. J.; Yang, Z.; Lu, Y. *J. Am. Chem. Soc.* **2005**, *127*, 12782–12783. (f) Kim, J.-M.; Chae, S. K.; Lee, Y. B.; Lee, J.-S.; Lee, G. S.; Kim, T.-Y.; Ahn, D. J. *Chem. Lett.* **2006**, *35*, 560–561. (g) Peng, H.; Tang, J.; Yang, L.; Pang, J.; Ashbaugh, H. S.; Brinker, C. J.; Yang, Z.; Lu, Y. *J. Am. Chem. Soc.* **2006**, *128*, 5304–5305. (h) Ahn, D. J.; Lee, S.; Kim, J.-M. *Adv. Funct. Mater.* **2008**, *18*, 1–14.
(21) (a) Mino, N.; Tamura, H.; Ogawa, K. *Langmuir* **1992**, *8*, 594–598. (b) Song, J.; Cheng, Q.; Kopta, S.; Stevens, R. C. *J. Am. Chem. Soc.* **2001**, *123*, 3205–3213.
(22) Kew, S. J.; Hall, E. A. H. *J. Mater. Chem.* **2006**, *16*, 2039–2047.
(23) (a) Charych, D. H.; Nagy, J. O.; Spevak, W.; Bednarski, M. D. *Science* **1993**, *261*, 585–588. (b) Reichert, A.; Nagy, J. O.; Spevak, W.; Charych, D. *J. Am. Chem. Soc.* **1995**, *117*, 829–830. (c) Ma, Z.; Li, J.; Liu, M.; Cao, J.; Zou, Z.; Tu, J.; Jiang, L. *J. Am. Chem.. Soc.* **1998**, *120*, 12678–12679. (d) Li, Y.; Ma, B.; Fan, Y.; Kong, X.; Li, J. *Anal. Chem.* **2002**, *74*, 6349–6354. (e) Orynbayeva, Z.; Kolusheva, S.; Livneh, E.; Lichtenshtein, A.; Nathan, I.; Jelinek, R. *Angew. Chem., Int. Ed.* **2005**, *44*, 1092–1096. (f) Ma, G.; Cheng, Q. *Langmuir* **2005**, *21*, 6123–6126. (g) Kim, J.-M.; Lee, Y. B.; Yang, D. H.; Lee, J.-S.; Lee, G. S.; Ahn, D. J. *J. Am. Chem. Soc.* **2005**, *127*, 17580–17581. (h) Nie, Q.; Zhang, Y.; Zhang, J.; Zhang, M. *J. Mater. Chem.* **2006**, *16*, 546–549. (i) Yoon, J.; Chae, S. K.; Kim, J.-M. *J. Am. Chem. Soc.* **2007**, *129*, 3038–3039. (j) Reppy, M. A.; Pindzola, B. A. *Chem. Commun.* **2007**, 4317–4338. (k) Lee, S.; Kim, J.-M. *Macromolecules* **2007**, *40*, 9201–9204. (l) Scindia, Y.; Silbert, L.; Volinsky, R.; Kolusheva, S.; Jelinek, R. *Langmuir* **2007**, *23*, 4682–4687.

terms of applications, the color transition of PDAs is being used to develop various types of sensors, so understanding these color changes should help improving on existing sensing devices. In this connection, for well-chosen side groups, dramatic color changes are observed when PDAs are subjected to an external stimulus such as stress,[19] heat,[10,16,20] pH change,[21] chemical change (dehydration),[22] interaction with chemicals and biochemicals.[20a−c,f−h,23] The color changes that are observed are typically from blue to red and vice versa, but other colors are known, especially purple.[17,24] The difference in fluorescence properties has also been utilized advantageously in PDA-based sensing materials.[23g,l,25] Finally, other detection schemes are possible, for instance, that different colors correspond to different Raman signatures.

Over the past few years, we have been engaged in a research program aimed at studying the spectroscopic properties of PDA chains isolated in their monomer single crystal matrix.[6] Red poly-3BCMU chains (poly-3BCMU = poly[4,6-decadiyne-1,10-diol bis([(*n*-butoxycarbonyl)methyl]urethane)]) have been shown to be perfect organic quantum wires on which electronic excitations are spatially coherent over the chain length, meaning that the excitations are states of the whole chain and are not localized on any specific part of it.[26−28] One can conjecture that this phenomenon should be observable for other CPs provided they can be obtained in the same very high degree of order as poly-3BCMU chains.

Red poly-3BCMU chains have an advantage which, at the same time, is a drawback: their very high dilution in the monomer crystal allows the study of a single chain; yet, red chains represent only a minority of all chains present in the crystal, the vast majority being blue chains. Consequently, many studies such as pump−probe experiments are precluded.[29−31]

We turned to other diacetylenes susceptible of producing exclusively red fluorescent PDA chains for three reasons: (i) to prove that the property of perfect quantum wire observed for poly-3BCMU chains is indeed general for red PDAs; (ii) to be able to study groups of red chains without interference from other types of chains; (iii) to prepare chains of different geometries in order to study the relationship between geometry and electronic properties, in the light of the assumption that blue chains are planar while all of the others are nonplanar, i.e., twisted. If so, different twist angles will lead to different electronic properties.

Scheme 2. Chemical Structure of 1,6-Bis(diphenylamino)-2,4-hexadiyne (THD)

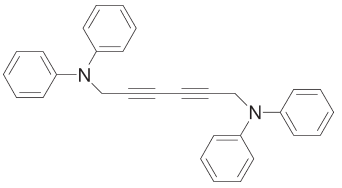

In this context, our goal was not to prepare another example of a PDA crystal containing 100% polymer, but to obtain a material where high-molecular-weight PDA chains would be diluted in their crystalline monomer matrix.

We first investigated a PDA named poly-THD (THD = 1,6-bis(diphenylamino)-2,4-hexadiyne, Scheme 2), one of the rare materials where nonplanar chains were found crystallographically. In this polymer, successive repeat units are alternatively rotated clockwise and anticlockwise with respect to the mean plane of the chain, resulting in a R−$C_4\cdots C_1$−R dihedral angle (see Scheme 1) of 166° (for planar chains this angle is 180°).[32] This PDA has been studied previously.[33−35] Its spectrocopic properties can be compared with those of poly-TCDU (poly-TCDU = poly-(5,7-decadiyne-1,12-diol-bis phenylurethane)), regarded in the past as a prototype for red PDAs,[36] and with those of isolated poly-3BCMU red chains.[6] The absorption maximum of the enyne backbone of poly-THD is observed at 568 nm (room temperature value);[33,37] it is red-shifted by comparison with that of poly-TCDU[38] ($\lambda_{max} \approx 530$ nm) and that of red poly-3BCMU[6] ($\lambda_{max} \approx 535$ nm). Still, its position is at a much higher energy than that of blue PDAs ($\lambda_{max} \approx$ 620 nm). Poly-THD is strongly fluorescent at low temperature but only weakly at room temperature because of the opening of a very efficient nonradiative decay channel.[37] In this respect, its behavior is quite similar to that of poly-3BCMU chains.

In a recent paper, it was shown that DFT calculations indeed find a minimum energy structure for poly-THD

(24) (a) Tieke, B.; Lieser, G. *Macromolecules* **1985**, *18*, 327–334. (b) Deckert, A. A.; Fallon, L.; Kiernan, L.; Cashin, C.; Perrone, A.; Encalarde, T. *Langmuir* **1994**, *10*, 1948–1954. (c) Deckert, A. A.; Horne, J. C.; Valentine, B.; Kiernan, L.; Fallon, L. *Langmuir* **1995**, *11*, 643–649. (d) Menzel, H.; Mowery, M. D.; Cai, M.; Evans, C. E. *J. Phys. Chem. B* **1998**, *102*, 9550–9556. (e) Carpick, R. W.; Sasaki, D. Y.; Marcus, M. S.; Eriksson, M. A.; Burns, A. R. *J. Phys.: Condens. Matter* **2004**, *16*, R679–R697. (f) Huang, X.; Jiang, S.; Liu, M. *J. Phys. Chem. B* **2005**, *109*, 114–119. (g) Dautel, O. J.; Robitzer, M.; Lère-Porte, J.-P.; Serein-Spirau, F.; Moreau, J. J. E. *J. Am. Chem. Soc.* **2006**, *128*, 16213–16223.
(25) Ryu, S.; Yoo, I.; Song, S.; Yoon, B.; Kim, J.-M. *J. Am. Chem. Soc.* **2009**, *131*, 3800–3801.
(26) Lécuiller, R.; Berréhar, J.; Ganière, J. D.; Lapersonne-Meyer, C.; Lavallard, P.; Schott, M. *Phys. Rev. B* **2002**, *66*, 125205−1–125205−6.
(27) Dubin, F.; Melet, R.; Barisien, T.; Grousson, R.; Legrand, L.; Schott, M.; Voliotis, V. *Nat. Phys.* **2006**, *2*, 32–35.
(28) Legrand, L.; Al Choueiry, A.; Holcman, J.; Enderlin, A.; Melet, R.; Barisien, T.; Voliotis, V.; Grousson, R.; Schott, M. *Phys. Status Solidi B* **2008**, *245*, 2702–2707.
(29) Kraabel, B.; Joffre, M.; Lapersonne-Meyer, C.; Schott, M. *Phys. Rev. B* **1998**, *58*, 15777–15788.
(30) Bigot, J.-Y.; Pham, T.-A.; Barisien, T. *Chem. Phys. Lett.* **1996**, *259*, 469–474.
(31) Yuasa, Y.; Ikuta, M.; Kobayashi, T.; Kimura, T.; Matsuda, H. *Phys. Rev. B* **2005**, *72*, 134302−1–134302−8.
(32) Enkelmann, V.; Schleier, G. *Acta Crystallogr., Sect. B* **1980**, *36*, 1954–1956.
(33) Morrow, M. E.; White, K. M.; Eckhardt, C. J.; Sandman, D. J. *Chem. Phys. Lett.* **1987**, *140*, 263–269.
(34) Agrinskaya, N. V.; Guk, E. G.; Kudryavtsev, I. A.; Lyublinskaya, O. G. *Phys. Solid State* **1995**, *37*, 526–529.
(35) Cholli, A. L.; Sandman, D. J.; Maas, W. *Macromolecules* **1999**, *32*, 4444–4446.
(36) Iqbal, Z.; Chance, R. R.; Baughman, R. H. *J. Chem. Phys.* **1977**, *66*, 5520–5525.
(37) Barisien, T.; Legrand, L.; Weiser, G.; Deschamps, J.; Balog, M.; Boury, B.; Dutremez, S. G.; Schott, M. *Chem. Phys. Lett.* **2007**, *444*, 309–313.
(38) Müller, H.; Eckhardt, C. J.; Chance, R. R.; Baughman, R. H. *Chem. Phys. Lett.* **1977**, *50*, 22–25.

Scheme 3. Chemical Structures of Diacetylenes 1−6

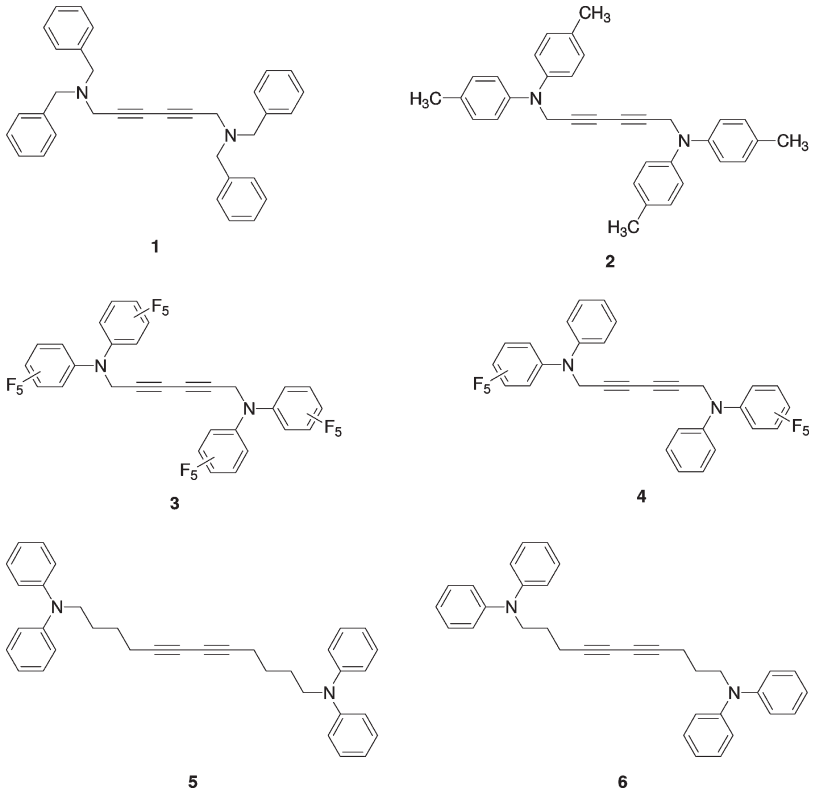

identical to the experimental one and, also, two other minima, one corresponding to a planar chain and the other to a much more twisted structure.[39] These two polymorphs have not been observed experimentally (although there are reports[40] of a surface phase in poly-THD crystals), and these findings suggest that other chain geometries might become accessible by a slight modification of the structure of the THD monomer.

Six THD analogues with slightly different side groups have been prepared (compounds **1**−**6** in Scheme 3), but only one of them, **6**, has a crystalline arrangement suitable for topochemical polymerization and is indeed reactive, and its polymer is soluble in common organic solvents. In effect, the crystal structures of these molecules result from a delicate balance between several types of weak interactions, some of them being intrastack and others interstack. When the leading interactions are intrastack, columnar assemblies are observed in which every other molecule is crystallographically equivalent (A−B−A−B arrangement). When the leading interactions are interstack, columnar assemblies are observed in which all of the molecules are crystallographically equivalent (A−A−A−A arrangement). The former arrangement is conducive to topochemical polymerization and the latter is not.

Polymerization of **6** is best performed by γ irradiation. The amount of polymer formed x_p increases linearly with the dose up to 25 MRad, at which stage $x_p \approx 0.18$. It would be possible to increase further the polymer contents (unless a phase transition to an inactive phase occurs at higher doses), but one would then reach a region where radiation damage becomes significant; typical G values for cross-linking or degradation are 0.5−2.[41] So, a structural study of a fully polymerized crystal is probably out of reach. Structural information about the polymer has been obtained in favorable cases by studying the structure of a polymer−monomer mixed crystal.[42−44] Such a study is planned.

Yet, in a first step, the computational method that was successful for poly-THD[39] was applied. Because it requires a 3D periodic system, a model ordered $(\mathbf{6})_{0.5}$-(poly-$\mathbf{6}$)$_{0.5}$ mixed crystal was studied, each chain being surrounded by four monomer stacks and each monomer stack by four chains (see Figure 6). The method and results are presented in the penultimate paragraph.

Results and Discussion

Preparation of Alkynes 7−12. Propargyl amines **7** and **8** (Scheme 4) were synthesized by allowing the parent amine to react with propargyl bromide in tetrahydrofuran (THF), with use of potassium hydroxide as a base and 18-crown-6 as a phase-transfer agent. Propargyl amines **9** and **10** were prepared similarly using potassium carbonate as a base

(39) Filhol, J.-S.; Deschamps, J.; Dutremez, S. G.; Boury, B.; Barisien, T.; Legrand, L.; Schott, M. *J. Am. Chem. Soc.* **2009**, *131*, 6976–6988.
(40) Hankin, S. H.; Sandman, D. J. *Macromolecules* **1991**, *24*, 4983–4984.
(41) Woods, R. J.; Pikaev, A. K. *Applied Radiation Chemistry: Radiation Processing*; Wiley-Interscience: New York, 1993.
(42) Day, D.; Lando, J. B. *J. Polym. Sci., Polym. Phys. Ed.* **1978**, *16*, 1009–1022.
(43) Foley, J. L.; Li, L.; Sandman, D. J.; Vela, M. J.; Foxman, B. M.; Albro, R.; Eckhardt, C. J. *J. Am. Chem. Soc.* **1999**, *121*, 7262–7263.
(44) Xu, R.; Schweizer, W. B.; Frauenrath, H. *J. Am. Chem. Soc.* **2008**, *130*, 11437–11445.

Scheme 4. Chemical Structures of Alkynes 7−14

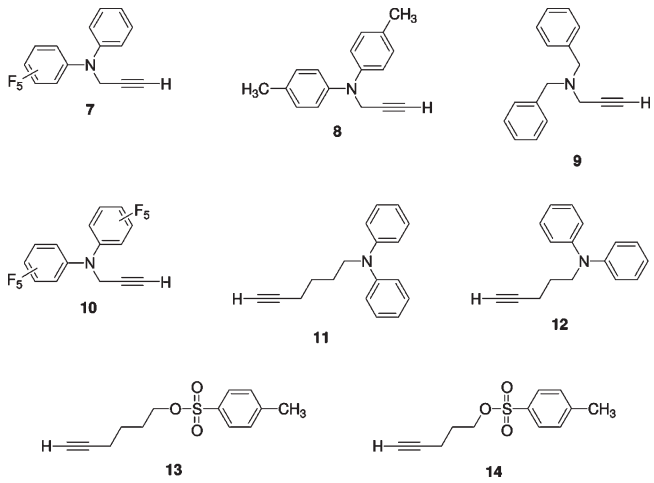

and, in the case of **10**, *N*,*N*-dimethylformamide (DMF) as a solvent; no 18-crown-6 was used. Propargyl amines **11** and **12** were obtained by allowing tosylated alkynes **13** and **14** to react with lithium diphenylamide in THF. Diphenylamine, dibenzylamine, and di-*p*-tolylamine were obtained from commercial sources. Bis(pentafluorophenyl)amine and (*N*-pentafluorophenyl)phenylamine were synthesized following reported methods.[45,46]

Syntheses of Diacetylenes 1−6. Symmetrical diynes **1**−**6** (Scheme 3) were synthesized by oxidative dimerization of alkynes **7**−**12** following the Hay coupling protocole.[47] For the syntheses of **1**−**4**, typically used acetone was replaced with methanol, and for the syntheses of **5** and **6**, acetone was replaced with 1,2-dimethoxyethane (DME).

Structure of 1,6-Bis(dibenzylamino)-2,4-hexadiyne (1). Diacetylene **1** crystallizes in the triclinic space group $P\bar{1}$ with $Z = 1$ (Table 1). There is one-half of a molecule in the asymmetric unit.[48] In the solid state (Figure 1), molecules of **1** pile up in stacks in the *a* direction. There are two short phenyl···phenyl contacts between molecules belonging to separate stacks. Edge-on interactions as those observed in strands of poly-THD are not present.[32] For the first contact, the H···Cg distance is 2.84 Å, the C−H···Cg angle 147.2°, and the angle between the H−Cg axis and the ring normal 2.97° (Cg is the centroid position of the phenyl ring). For the second contact, the H···Cg distance is 2.99 Å, the C−H···Cg angle 131.7°, and the angle between the H−Cg axis and the ring normal 12.89°. These interactions are of type III according to Malone's classification, that is, the C−H vector faces in an oblique fashion the phenyl ring it interacts with and the hydrogen atom sits nearly above the center of gravity of the phenyl ring.[49] The H···Cg distances found here are slightly longer than the average one reported in the literature (2.76 Å), suggesting weaker C_{arom}−H···π interactions.[50] There is also one short contact between a CH_2 hydrogen and an aromatic carbon atom (d(H···C_{arom}) = 2.881 Å, ∠C−H···C_{arom} = 159.9°).

Two consecutive molecules in a given stack are separated by a distance of 5.539 Å. This distance rules out significant intrastack π···π interactions.[51−53] Stronger, yet still weak, π···π interactions are observed between phenyl rings from separate stacks. In this case, the centroid···centroid distance is 4.211 Å and the angle between the centroid-centroid vector and the ring normal 28.44°. This primary OFF interaction combined with the 2.99 Å C_{arom}−H···π contact discussed previously generates a pattern that is reminiscent of the P4AE (parallel 4-fold aryl embrace) secondary motif found in metal phenanthroline complexes.[54]

Structure of 1,6-Bis(di-*p*-tolylamino)-2,4-hexadiyne (2). Diacetylene **2** crystallizes in the triclinic space group $P\bar{1}$ with $Z = 1$ (Table 1). There is one-half of a molecule in the asymmetric unit.[48] In the solid state (Figure 2), molecules of **2** pile up in stacks in the *a* direction. There are no short C_{arom}−H···aryl contacts. The only short contacts that are observed are CH_2···aryl, CH_3···aryl, and C_{arom}−H···C_{sp} interactions. For the first interaction, the H···Cg distance is 2.64 Å, the C−H···Cg angle 147.3°, and the angle between the H−Cg axis and the ring normal 4.65° (Cg is the centroid position of the aryl group). For the second contact, the H···Cg distance is 2.95 Å, the C−H···Cg angle 151.5°, and the angle between the H−Cg axis and the ring normal 5.26°. For the third interaction, the H···C_{sp} distance is 2.895 Å and the C_{arom}−H···C_{sp} angle 145.7°.

Two consecutive molecules in a given stack are separated by a distance of 6.127 Å. This distance rules out significant intrastack π···π interactions.[51−53] There is one offset face-to-face π···π interaction between aryl groups from separate stacks, yet this interaction is quite weak: the centroid···centroid distance is 4.897 Å and the angle between the centroid−centroid vector and the ring normal 31.81°. This primary OFF interaction combined with the CH_3···aryl contact discussed previously generates here again a pattern that is reminiscent of the P4AE secondary motif found in metal phenanthroline complexes.[54] Unlike the situation found in **1**, however, the assembly is looser.

Structure of 1,6-Bis(dipentafluorophenylamino)-2,4-hexadiyne (3). Compound **3** crystallizes in the monoclinic space group $P2_1/n$ with $Z = 2$ (Table 1). In the unit cell, the molecule sits on a center of inversion.[48] Molecules of **3** pile

(45) Koppang, R. *Acta Chem. Scand.* **1971**, *25*, 3067–3071.
(46) Koppang, R. *J. Fluorine Chem.* **1995**, *74*, 177–179.
(47) (a) Hay, A. S. *J. Org. Chem.* **1962**, *27*, 3320–3321. (b) Walton, D. R. M.; Waugh, F. *J. Organomet. Chem.* **1972**, *37*, 45–56. (c) Eastmond, R.; Johnson, T. R.; Walton, D. R. M. *Tetrahedron* **1972**, *28*, 4601–4616. (d) Ghose, B. N. *Synth. React. Inorg. Met.-Org. Chem.* **1994**, *24*, 29–52. (e) Brandsma, L. *Studies in Organic Chemistry 34: Preparative Acetylenic Chemistry*, 2nd ed.; Elsevier: Amsterdam, 1988; p 219.
(48) CCDC-746114 (**1**), CCDC-746116 (**2**), CCDC-746111 (**3**), CCDC-746112 (**4**), CCDC-746115 (**5**), and CCDC-746113 (**6**) contain the supplementary crystallographic data for this paper. These data can be obtained free of charge from the Cambridge Crystallographic Data Centre via www.ccdc.cam.ac.uk/data_request/cif.
(49) Malone, J. F.; Murray, C. M.; Charlton, M. H.; Docherty, R.; Lavery, A. J. *J. Chem. Soc., Faraday Trans.* **1997**, *93*, 3429–3436.
(50) Umezawa, Y.; Tsuboyama, S.; Honda, K.; Uzawa, J.; Nishio, M. *Bull. Chem. Soc. Jpn.* **1998**, *71*, 1207–1213.
(51) Moon, H.; Zeis, R.; Borkent, E.-J.; Besnard, C.; Lovinger, A. J.; Siegrist, T.; Kloc, C.; Bao, Z. *J. Am. Chem. Soc.* **2004**, *126*, 15322–15323.
(52) Sokolov, A. N.; Friščić, T.; MacGillivray, L. R. *J. Am. Chem. Soc.* **2006**, *128*, 2806–2807.
(53) Janiak, C. *J. Chem. Soc., Dalton Trans.* **2000**, 3885–3896.
(54) (a) Russell, V.; Scudder, M.; Dance, I. *J. Chem. Soc., Dalton Trans.* **2001**, 789–799. (b) Dance, I. *CrystEngComm* **2003**, *5*, 208–221.

Table 1. Crystal Data and Experimental Details of Data Collection and Refinement for Compounds 1−6

	1	2	3	4	5	6
empirical formula	$C_{34}H_{32}N_2$	$C_{34}H_{32}N_2$	$C_{30}H_4F_{20}N_2$	$C_{30}H_{14}F_{10}N_2$	$C_{36}H_{36}N_2$	$C_{34}H_{32}N_2$
fw	468.64	468.64	772.35	592.43	496.70	468.62
cryst color and habit	colorless rod	colorless block	colorless stick	colorless plate	colorless prism	colorless platelet
cryst size (mm^3)	0.12 × 0.15 × 0.35	0.15 × 0.16 × 0.45	0.05 × 0.12 × 0.50	0.02 × 0.06 × 0.30	0.28 × 0.30 × 0.50	0.05 × 0.15 × 0.20
cryst syst	triclinic	triclinic	monoclinic	monoclinic	triclinic	monoclinic
space group	$P\bar{1}$ (No. 2)	$P\bar{1}$ (No. 2)	$P2_1/n$ (No. 14)	$P2_1/n$ (No. 14)	$P\bar{1}$ (No. 2)	$P2_1/n$ (No. 14)
a (Å)	5.5393(8)	6.1269(11)	5.6906(10)	20.947(6)	8.3279(8)	9.9484(7)
b (Å)	9.8301(10)	9.5278(11)	8.920(3)	6.109(2)	10.1420(10)	16.0893(12)
c (Å)	13.3335(13)	12.720(2)	27.215(7)	22.286(6)	17.6024(17)	16.7643(13)
α (deg)	68.610(9)	103.70(1)	90	90	90.294(8)	90
β (deg)	79.331(8)	102.77(1)	96.690(18)	95.38(3)	101.661(8)	98.697(4)
γ (deg)	87.370(10)	102.73(1)	90	90	100.022(8)	90
V ($Å^3$)	664.15(14)	673.78(19)	1372.0(6)	2839.3(15)	1432.6(2)	2652.5(3)
Z	1	1	2	4	2	4
T (K)	173	173	173	173	173	180
ρ_{calcd} (g cm^{-3})	1.172	1.155	1.869	1.386	1.151	1.173
$F(000)$	250	250	756	1192	532	1000
μ (mm^{-1})	0.68	0.67	2.07	1.28	0.66	0.68
T_{min}, T_{max}	0.93, 0.97	0.82721, 1.00000	0.97, 0.99	0.99, 1.00	0.88622, 1.00000	0.902, 0.988
graphite-monochromated $Mo_{K\alpha}$ radiation (Å)	0.71073	0.71073	0.71073	0.71073	0.71073	0.71073
θ range (deg)	3.2241−32.1630	3.259−32.437	2.736−32.451	2.803−32.381	2.959−32.422	1.76−26.37
index ranges	$-8 \le h \le 8$, $-14 \le k \le 13$, $-19 \le l \le 19$	$-8 \le h \le 9$, $-14 \le k \le 14$, $-19 \le l \le 18$	$-8 \le h \le 7$, $-13 \le k \le 12$, $-40 \le l \le 38$	$-30 \le h \le 30$, $-9 \le k \le 8$, $-32 \le l \le 33$	$-11 \le h \le 11$, $-13 \le k \le 14$, $-25 \le l \le 25$	$-12 \le h \le 12$, $-20 \le k \le 20$, $-18 \le l \le 20$
data collected	11220	11512	23485	48109	24260	29768
unique data, R_{int}	4247, 0.021	4270, 0.027	4520, 0.025	9058, 0.139	9020, 0.026	5425, 0.0333
obsd data ($I_o > n\sigma(I_o)$)	1399 (n = 3)	1813 (n = 2)	980 (n = 2)	551 (n = 2)	3682 (n = 2)	4037 (n = 2)
L.S. params, restraints	163, 0	163, 0	235, 0	169, 0	343, 0	325, 0
R,[a] R_w[b] (obsd reflns)	0.0365, 0.0381	0.0368, 0.0404	0.0217, 0.0220	0.1001, 0.0966	0.0346, 0.0379	0.0389, 0.0842
R,[a] R_w[b] (all reflns)	0.1281, 0.0475	0.0949, 0.0540	0.1658, 0.0406	0.4767, 0.2014	0.0997, 0.0799	0.0617, 0.0948
weighting scheme[c,d]	28.7, −44.6, 25.3, −9.62	3.26, −1.88, 3.71, −0.758, 0.999	12.8, −18.4, 15.0, −6.02, 2.95	14.0, −10.2, 11.1	3.91, −0.963, 2.32	0.0379, 0.6852
max shift/esd	0.000121	0.000145	0.002431	0.006548	0.009629	0.001
GOF	1.0363	1.1305	1.2424	1.1211	1.1048	1.021
$\Delta\rho_{min}$, $\Delta\rho_{max}$ (e $Å^{-3}$)	−0.17, 0.16	−0.16, 0.17	−0.14, 0.14	−0.56, 1.02	−0.16, 0.19	−0.2, 0.189

[a] $R = \Sigma\,||F_o| - |F_c||/\Sigma\,|F_o|$. [b] $R_w = [\Sigma\,(w\,(F_o^2 - F_c^2)^2)/\Sigma\,(w\,(F_o^2)^2)]^{1/2}$. [c] For compounds **1**−**5**, w = [weight][1 − $(\Delta F/6\sigma(F))^2$]^2; [weight] = 1.0/$[A_0T_0(x) + A_1T_1(x) + \ldots + A_{n-1}T_{n-1}(x)]$ where A_i are the Chebychev coefficients listed in the Table and $x = F_{calcd}/F_{max}$. [d] For diacetylene **6**, w = $1/[\sigma^2(F_o^2) + (aP)^2 + bP]$; $P = (F_o^2 + 2F_c^2)/3$, and the values of a and b are given in the Table.

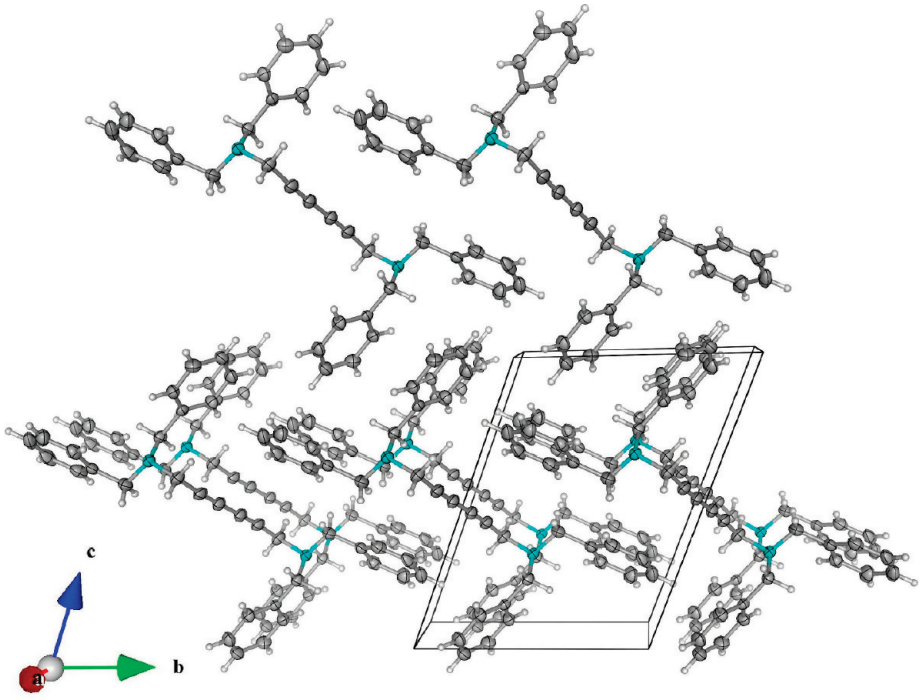

Figure 1. View along the *a* axis showing the organization of **1** in the crystalline state.

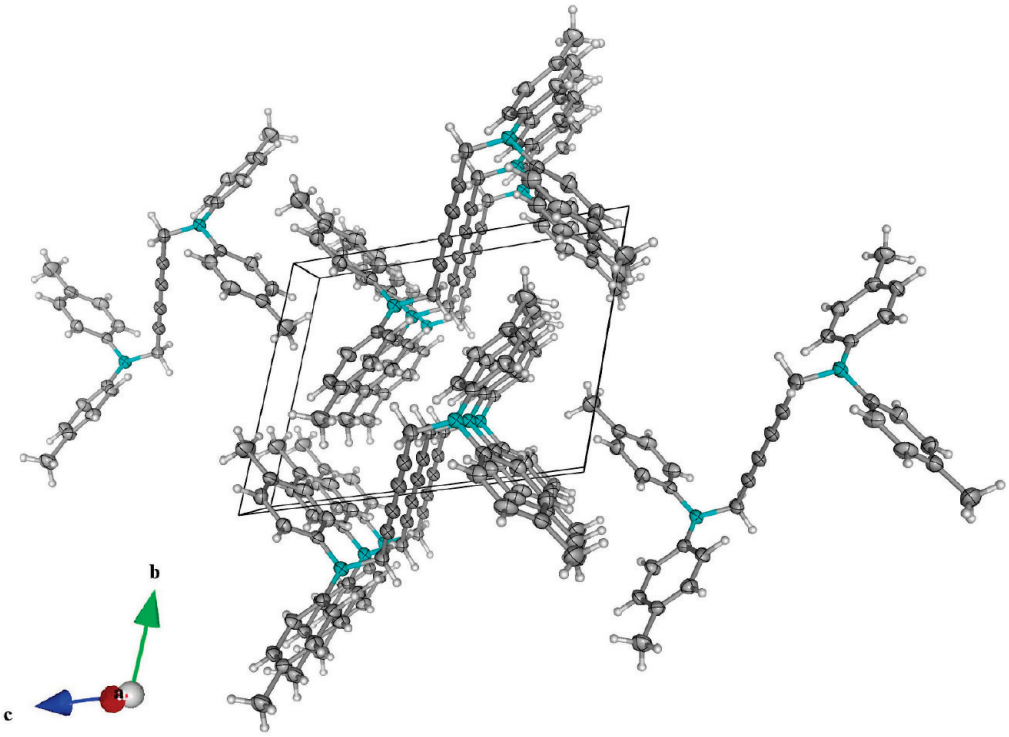

Figure 2. View along the *a* axis showing the organization of **2** in the crystalline state.

up in stacks in the *a* direction (Figure 3). Two consecutive molecules in a given stack are separated by a distance of 5.691 Å. Such a long distance precludes significant $\pi\cdots\pi$ interaction.[51−53] There is one offset face-to-face $\pi\cdots\pi$ interaction between pentafluorophenyl rings from separate stacks, yet this interaction is quite weak: the centroid$\cdots$centroid distance is 4.912 Å and the angle between the centroid-centroid vector and the ring normal 50.39°.

The structure exhibits numerous C−F$\cdots$$C_{aryl}$, C−F$\cdots$$C_{sp}$, C−F$\cdots$F, and C−H$\cdots$F interactions between molecules from separate stacks.[55] There are eight different C−F$\cdots$$C_{aryl}$ contacts spanning the range 3.095−3.162 Å. There is one C−F$\cdots$$C_{sp}$ contact for which the F$\cdots$$C_{sp}$ distance is 2.979 Å. There are three different C−F$\cdots$F contacts for which d(F$\cdots$F) = 2.722, 2.904, and 2.907 Å. There are two distinct C−H$\cdots$F interactions for which d(H$\cdots$F) = 2.616 and 2.638 Å.

Structure of 1,6-Bis((*N*-pentafluorophenyl)phenylamino)-2,4-hexadiyne (4). Compound **4** crystallizes in the monoclinic space group $P2_1/n$ with Z = 4 (Table 1). There is one molecule per asymmetric unit.[48] Molecules of **4** pile up in stacks in the *b* direction (Figure 4). Two consecutive molecules in a given stack are separated by a distance of 6.109 Å. Such a long distance precludes significant intrastack $\pi\cdots\pi$ interaction.[51−53] The shortest $\pi\cdots\pi$ interaction is observed between a phenyl ring and a pentafluorophenyl group from a different stack. In this case, the centroid$\cdots$centroid distance is 4.783 Å and the angle between the centroid-centroid vector and the ring normal 19.78°. This interaction is different from the phenyl$\cdots$perfluorophenyl face-to-face stacking interaction typically observed in single-component organic molecules or cocrystals in which both groups are present.[56] Interestingly, segregation prevails in

(55) (a) Thalladi, V. R.; Weiss, H.-C.; Bläser, D.; Boese, R.; Nangia, A.; Desiraju, G. R. *J. Am. Chem. Soc.* **1998**, *120*, 8702–8710. (b) Renak, M. L.; Bartholomew, G. P.; Wang, S.; Ricatto, P. J.; Lachicotte, R. J.; Bazan, G. C. *J. Am. Chem. Soc.* **1999**, *121*, 7787–7799. (c) Dai, C.; Nguyen, P.; Marder, T. B.; Scott, A. J.; Clegg, W.; Viney, C. *Chem. Commun.* **1999**, 2493–2494. (d) Lorenzo, S.; Lewis, G. R.; Dance, I. *New J. Chem.* **2000**, *24*, 295–304. (e) Adams, N.; Cowley, A. R.; Dubberley, S. R.; Sealey, A. J.; Skinner, M. E. G.; Mountford, P. *Chem. Commun.* **2001**, 2738–2739. (f) Hair, G. S.; Cowley, A. H.; Gorden, J. D.; Jones, J. N.; Jones, R. A.; Macdonald, C. L. B. *Chem. Commun.* **2003**, 424–425.

(56) (a) Naae, D. G. *Acta Crystallogr., Sect. B* **1979**, *35*, 2765–2768. (b) Williams, J. H. *Acc. Chem. Res.* **1993**, *26*, 593–598. (c) Coates, G. W.; Dunn, A. R.; Henling, L. M.; Dougherty, D. A.; Grubbs, R. H. *Angew. Chem., Int. Ed.* **1997**, *36*, 248–251. (d) Coates, G. W.; Dunn, A. R.; Henling, L. M.; Ziller, J. W.; Lobkovsky, E. B.; Grubbs, R. H. *J. Am. Chem. Soc.* **1998**, *120*, 3641–3649. (e) Ponzini, F.; Zagha, R.; Hardcastle, K.; Siegel, J. S. *Angew. Chem., Int. Ed.* **2000**, *39*, 2323–2325. (f) Liu, J.; Murray, E. M.; Young, V. G., Jr. *Chem. Commun.* **2003**, 1904–1905. (g) Meyer, E. A.; Castellano, R. K.; Diederich, F. *Angew. Chem., Int. Ed.* **2003**, *42*, 1210–1250. (h) Smith, C. E.; Smith, P. S.; Thomas, R. Ll.; Robins, E. G.; Collings, J. C.; Dai, C.; Scott, A. J.; Borwick, S.; Batsanov, A. S.; Watt, S. W.; Clark, S. J.; Viney, C.; Howard, J. A. K.; Clegg, W.; Marder, T. B. *J. Mater. Chem.* **2004**, *14*, 413–420. (i) Watt, S. W.; Dai, C.; Scott, A. J.; Burke, J. M.; Thomas, R. Ll.; Collings, J. C.; Viney, C.; Clegg, W.; Marder, T. B. *Angew. Chem., Int. Ed.* **2004**, *43*, 3061–3063. (j) Xu, R.; Gramlich, V.; Frauenrath, H. *J. Am. Chem. Soc.* **2006**, *128*, 5541–5547.

(57) (a) Cox, E. G.; Cruickshank, D. W. J.; Smith, J. A. S. *Proc. R. Soc. London, Ser. A* **1958**, *247*, 1–21. (b) Burley, S. K.; Petsko, G. A. *Science* **1985**, *229*, 23–28. (c) Perutz, M. F.; Fermi, G.; Abraham, D. J.; Poyart, C.; Bursaux, E. *J. Am. Chem. Soc.* **1986**, *108*, 1064–1078. (d) Burley, S. K.; Petsko, G. A. *J. Am. Chem. Soc.* **1986**, *108*, 7995–8001. (e) Askew, B.; Ballester, P.; Buhr, C.; Jeong, K. S.; Jones, S.; Parris, K.; Williams, K.; Rebek, J., Jr. *J. Am. Chem. Soc.* **1989**, *111*, 1082–1090. (f) Jorgensen, W. L.; Severance, D. L. *J. Am. Chem. Soc.* **1990**, *112*, 4768–4774. (g) Hunter, C. A.; Sanders, J. K. M. *J. Am. Chem. Soc.* **1990**, *112*, 5525–5534. (h) Hunter, C. A. *Chem. Soc. Rev.* **1994**, *23*, 101–109. (i) Dougherty, D. A. In *Molecular Recognition: Receptors for Molecular Guests*; Vögtle, F., Ed.; Comprehensive Supramolecular Chemistry; Pergamon: London, 1996; Vol. *2*, Chapter 6, pp 195−209. (j) Weiss, H.-C.; Bläser, D.; Boese, R.; Doughan, B. M.; Haley, M. M. *Chem. Commun.* **1997**, 1703–1704.

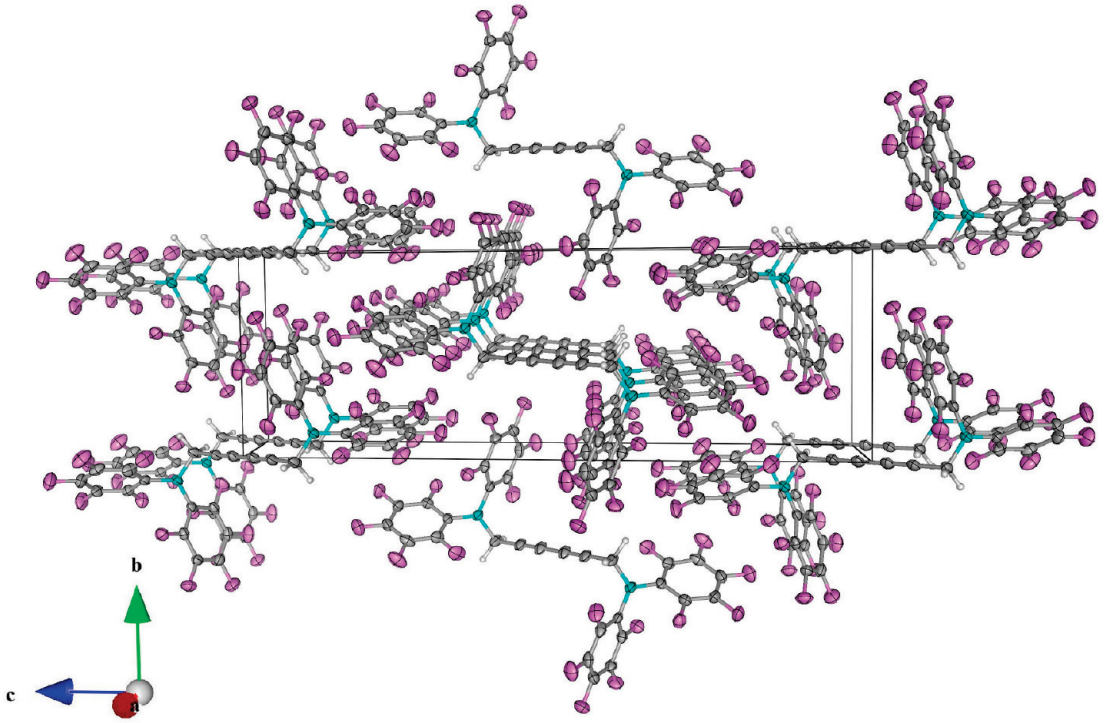

Figure 3. View along the *a* axis showing the organization of **3** in the crystalline state.

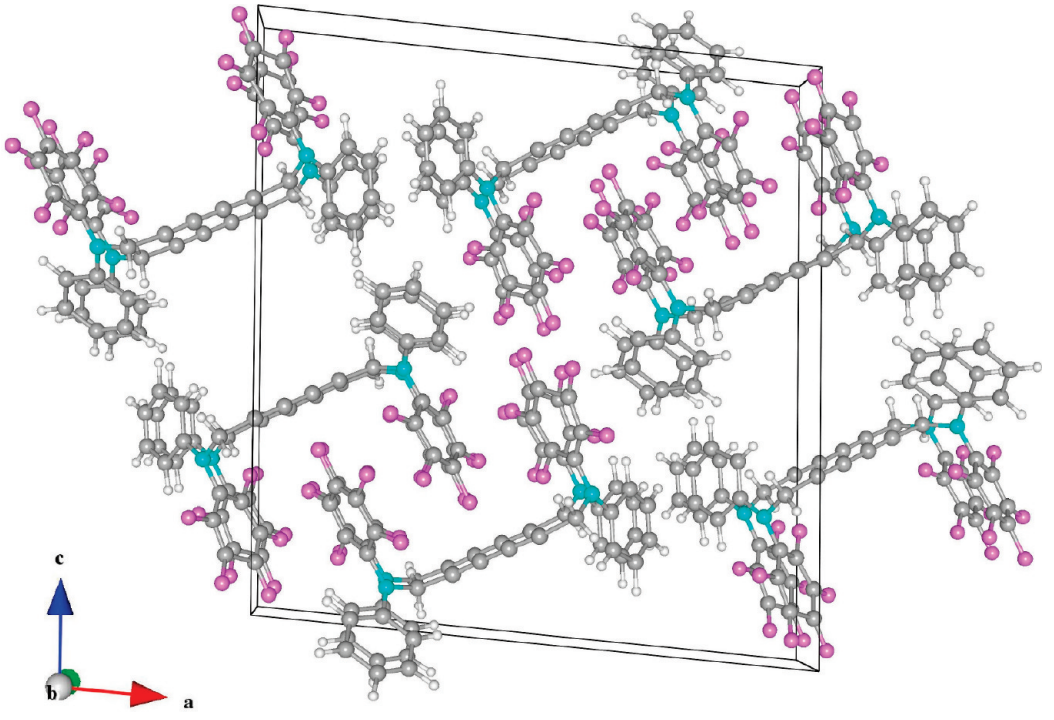

Figure 4. View along the *b* axis showing the organization of **4** in the crystalline state.

the structure of **4**: phenyl groups stack on top of one another, and the same is true for pentafluorophenyl groups.

The structure exhibits numerous C−F···C_{aryl}, C−F···F, C_{arom}−H···F, CH_2···F, and C_{arom}−H···phenyl interactions between molecules from separate stacks.[55,57] The two distinct C−F···C_{aryl} contacts have distances of 3.111 and 3.116 Å and the two C−F···F contacts of 2.623 and 2.736 Å. There are three different C_{arom}−H···F interactions for which d(H···F) = 2.456, 2.659, and 2.662 Å. The lengths of the two separate CH_2···F contacts are 2.271 and 2.464 Å. There is one edge-to-face C−H···π interaction between nearby phenyl rings: the H(54)−C(29)−C(30)−H(55) fragment of the first ring interacts with the C(31′) and C(29′) carbon atoms of the second ring. In this case, the C(29)−H(54)···C(31′) distance is 2.772 Å and the C(30)−H(55)···C(29′) distance 2.952 Å.

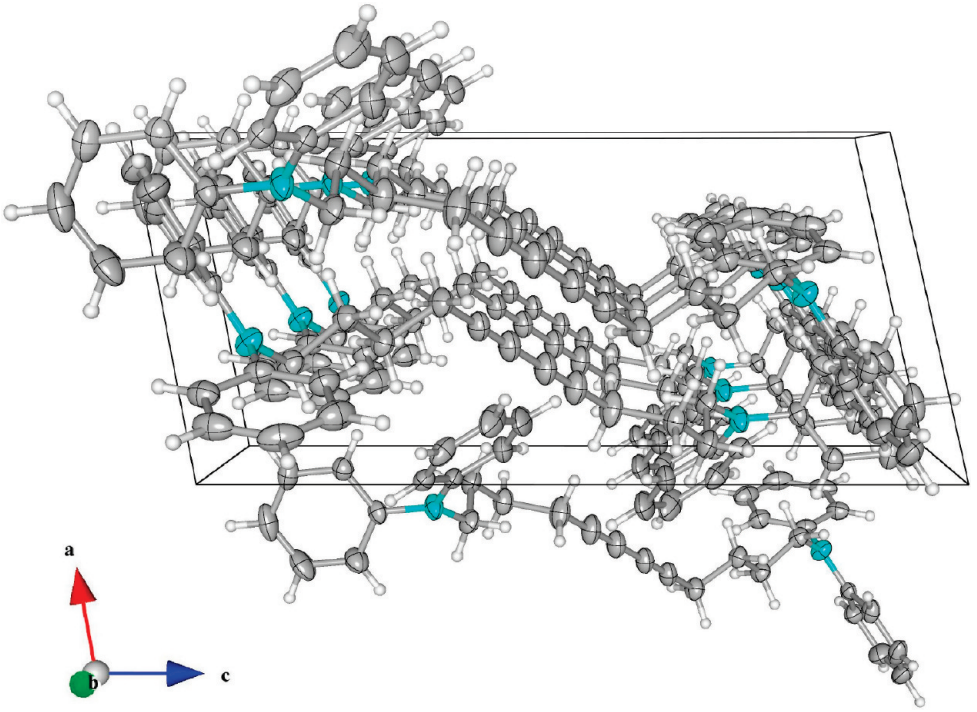

Figure 5. View along the *b* axis showing the organization of **5** in the crystalline state.

Structure of 1,12-Bis(diphenylamino)-5,7-dodecadiyne (5). Compound **5** crystallizes in the triclinic space group $P\bar{1}$ with $Z = 2$ (Table 1). There is one entire molecule in the asymmetric unit.[48] The structure exhibits numerous phenyl···phenyl interactions (Figure 5). There are two phenyl···phenyl interactions with geometries resembling tilted T structures. For these interactions, the H···Cg distances and C−H···Cg angles (Cg is the centroid position of the phenyl ring) are as follows: 3.131 Å (161.74°), 3.169 Å (140.18°). There are three other phenyl···phenyl interactions with geometries resembling tilted T structures but, in these cases, the C−H vector points to a specific aromatic carbon atom rather than to the phenyl centroid. The H···C_{arom} distances, along with the corresponding C_{arom}-H···C_{arom} angles, are as follows: 2.803 Å (161.60°), 2.866 Å (148.85°), 2.884 Å (122.82°). There are two edge-to-face C−H···π interactions between phenyl rings. In the first edge-to-face interaction, the H(45)−C(10)−C(9)−H(44) fragment interacts with the C(2)−C(3) edge of the C(1)−C(2)−C(3)−C(4)−C(5)−C(6) phenyl ring. In this case, the H(45)···C(3) distance is 2.885 Å and the H(44)···C(2) distance 3.266 Å. In the second edge-to-face interaction, the H(40)−C(4)−C(5)−H(39) fragment interacts with the C(33)−C(34)−C(35)−C(36)−C(37)−C(38) phenyl ring (d(H(40)···C(35)) = 2.956 Å and d(H(39)···C(38)) = 3.348 Å). These edge-on interactions are quite similar to those observed in poly-THD.[32] There is also one short CH_2···C_{sp} contact (d(H···C_{sp}) = 2.798 Å, ∠C−H···C_{sp} = 163.21°) and one short CH_2···phenyl contact (d(H···Cg) = 2.792 Å, ∠C−H···Cg = 159.27°).

Structure of 1,10-Bis(diphenylamino)-4,6-decadiyne (6). Compound **6** crystallizes in the monoclinic space group $P2_1/n$ with $Z = 4$ (Table 1). There is one entire molecule in the asymmetric unit.[48] The structure is sustained by numerous phenyl···phenyl interactions (Figure 6). There are two phenyl···phenyl interactions with geometries resembling tilted T structures. For these interactions, the H···Cg distances and C−H···Cg angles (Cg is the centroid position of the phenyl ring) are as follows: 2.799 Å (160.41°), 2.866 Å (149.82°). There are two edge-to-face C−H···π interactions between phenyl rings. In the first edge-to-face interaction, the H(34)−C(34)−C(35)−H(35) fragment interacts with the C(11)−C(12)−C(13)−C(14)−C(15)−C(16) phenyl ring (d(H(34)···C(14)) = 3.117 Å and d(H(35)···C(11)) = 2.993 Å). In the second edge-to-face interaction, the H(18)−C(18)−C(20)−H(20) fragment interacts with the C(24)−C(25)−C(26)−C(27)−C(28)−C(29) phenyl ring (d(H(18)···C(24)) = 3.024 Å and d(H(20)···C(27)) = 3.102 Å). Here again, these edge-to-face interactions resemble those found in poly-THD.[32] There are two short C_{arom}−H···C_{arom} interactions with no specific geometries for which d(H···C_{arom}) = 2.873 Å and ∠C_{arom}−H···C_{arom} = 140.68°, and d(H···C_{arom}) = 2.876 Å and ∠C_{arom}−H···C_{arom} = 137.84°. Three short CH_2···C_{sp} contacts are observed with the following geometrical parameters: d(H···C_{sp}) = 2.721 Å and ∠C−H···C_{sp} = 147.99°, d(H···C_{sp}) = 2.816 Å and ∠C−H···C_{sp} = 132.28°, and d(H···C_{sp}) = 2.895 Å and ∠C−H···C_{sp} = 125.08°. Also, there is one short C_{arom}−H···C_{sp} contact for which d(H···C_{sp}) = 2.894 Å and ∠C_{arom}−H···C_{sp} = 153.22°.

1,10-Bis(diphenylamino)-4,6-decadiyne (6): A New Polymerizable Diacetylene. Close examination of the packings of **1**, **2**, **3**, and **4** indicates that the molecules are not suitably oriented for topochemical polymerization. The geometrical parameters d, R_v, and γ (see Table 2) differ significantly from Baughman's criteria for topochemical polymerization (vide supra).

Molecules of **5** pile up in columns in the *b* direction. In each column, the distance between two consecutive molecules is

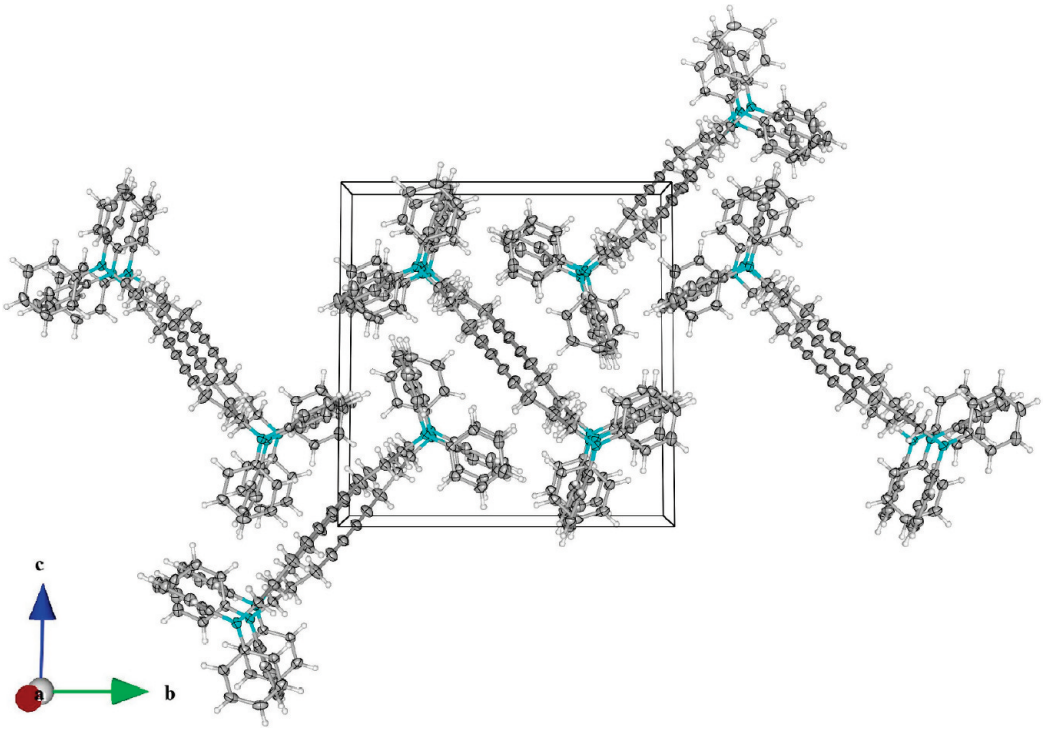

Figure 6. View along the *a* axis showing the organization of **6** in the crystalline state.

10.142 Å. Such a long distance makes polymerization along an axis passing through the centers of the molecules unlikely. Interestingly, polymerization appears to be possible along an axis that runs parallel to the *b* direction and is located in the middle of two stacks, i.e. passing through a center of inversion of the unit cell (Figure 5). In this way, two stacks combine into a bigger one; in this bigger stack, reacting molecules are closer and alternate sides along the polymerization axis. This situation resembles a "wrinkled carpet".

Looking down the polymerization axis, all of the odd-numbered molecules are crystallographically equivalent, and the same is true for even-numbered molecules. As a result, two sets of geometrical parameters must be considered to determine whether topochemical polymerization is possible. For the first set of possibly reacting molecules, the stacking distance *d* (Scheme 1) is 5.818 Å, and the perpendicular distance R_v is 3.7670 Å. The γ angle between a diacetylene rod and an axis passing through the centers of the molecules is 40.21°. For the second set of molecules, the stacking distance *d* is 5.192 Å, and the perpendicular distance R_v is 4.1834 Å. The γ angle between a diacetylene rod and an axis passing through the centers of the molecules is 53.61°. These geometrical parameters do not match Baughman's criteria for topochemical polymerization although they are close (vide supra).

Molecules of **6** pile up in columns in the *a* direction (Figure 6). The axes of the columns are all parallel but the stacks are not aligned identically: each column is sandwiched perpendicularly by two other columns. The C≡C−C≡C fragments of the molecules in the central stack face the NPh_2 parts of the molecules from the contiguous stacks. A similar situation was not observed in **5**.

Table 2. Geometrical Parameters for Diacetylenes 1−6[a]

compd	*d* (Å)	R_v (Å)	γ (deg)
1	5.539	3.60	39.9
2	6.127	4.155	42.6
3	5.691	4.506	52.36
4	6.109	5.554	66.56
5	5.192	4.1834	53.61
	5.818	3.7670	40.21
6	4.937	3.4946	45.36
	5.281	3.573	41.39

[a] *d*, R_v, and γ are defined in Scheme 1.

Similarly to **5**, the polymerization axis cannot encompass the centers of all of the C≡C−C≡C fragments in each stack and must be located in-between them. It is parallel to the *a* axis and goes through a center of inversion of the unit cell. It follows that two sets of geometrical parameters must be considered to determine whether topochemical polymerization is possible. For the first group of possibly reacting molecules (odd−even couple), the stacking distance *d* (Scheme 1) is 4.937 Å, and the perpendicular distance R_v is 3.4946 Å. The γ angle between a diacetylene rod and an axis passing through the centers of the molecules is 45.36°. For the second group of molecules (even−odd couple), the stacking distance *d* is 5.281 Å, and the perpendicular distance R_v is 3.573 Å. The γ angle between a diacetylene rod and an axis passing through the centers of the molecules is 41.39°. The first set of geometrical parameters thus matches perfectly Baughman's criteria for topochemical polymerization and the second one is quite close (vide supra).

It is noteworthy that the crystal structure of **6** is at 180 K, whereas polymerization is carried out at or near room temperature. Nevertheless, this situation does not introduce

any significant error. Indeed, spectroscopic studies (vide infra) show smooth and modest variations between these two temperatures, indicative of the absence of any phase transition. Furthermore, thermal expansion is estimated to be about 1% considering typical expansion coefficients for van der Waals crystals, such changes being too small to grossly affect the geometry of the reacting centers.

In conclusion, the presence of $C_{arom}-H\cdots\pi$ interactions between molecules susceptible of getting linked via topochemical polymerization is essential to obtain a reactive THD analogue. These interactions contribute to generating columnar assemblies with an A−B−A−B type arrangement in which each molecule is shifted sideways with respect to the two surrounding ones along the polymerization axis. Such interactions are present in the crystal structures of **5** and **6**. Yet, the longer hydrocarbon spacer between the C≡C−C≡C fragment and the NPh_2 group in **5** makes this latter diacetylene unreactive. Thus, by a slight modification of the length of this spacer, it is possible to fine-tune the reactivity of THD analogues. Modifications of the THD skeleton resulting in the loss of these intracolumn $C_{arom}-H\cdots\pi$ interactions lead to unreactive monomers. This is observed for diacetylenes **1**−**4**. In these diacetylenes, the leading interactions are interstack, so these contacts do not contribute to making possibly reacting molecules closer. In **1**−**4**, columns with an A−A−A−A arrangement are observed in which all of the molecules are equivalent and lie far apart.

Polymerization Studies. Among the six DAs studied in this work, compound **6** is the only one for which crystallography suggests that topochemical polymerization should be possible. We show thereafter that this diacetylene indeed polymerizes in the solid state, thermally and photochemically (UV and γ). The resulting PDA, poly-**6**, has been characterized spectroscopically in the solid state, and because this polymer is soluble in organic solvents, solution studies have also been carried out.

Absorption Studies of Poly-6 and Molecular Weight Determination. Figure 7 shows the UV−visible absorption spectrum of a chloroform solution of the polymer at a concentration of 0.05 mg mL^{-1}. A structureless band is observed at $\lambda_{max} \approx 470$ nm that is absent from the spectrum of the nonirradiated monomer. Previous studies on solutions of neutral PDAs have shown a similar absorption band.[58] This band is characteristic of the so-called yellow state of PDAs in good solvents, that is solvents in which the macromolecules are isolated, coiled, worm-like chains.[58c,59] From absorption spectra such as the one shown in Figure 7, it is possible to calculate the extinction coefficient of the polymer in a good solvent at λ_{max}, in this case $\alpha = 40200 \pm 1500$ L mol^{-1} cm^{-1}; this

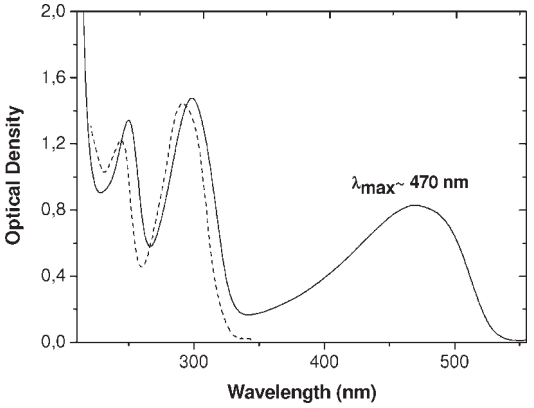

Figure 7. Room temperature absorption spectrum of a chloroform solution of pure poly-**6** at a concentration of 0.05 mg mL^{-1} (solid line). The dashed line corresponds to the absorption spectrum of *N*-methyldiphenylamine at 20 °C in methylcyclohexane (data from Förster et al.[61]).

value is typical of PDAs in a yellow solution.[58a,60] Two additional bands are observed around 250 and 300 nm in Figure 7 that originate from the side groups of poly-**6**; the positions of these bands compare well with those of *N*-methyldiphenylamine in methylcyclohexane solution (dashed line).[61]

A number average molecular weight, M_n, of 300 000 Da was found experimentally by size exclusion chromatography (SEC) for poly-**6** dissolved in THF, with use of commonly employed polystyrene calibration. However, it has been observed for some PDAs that this calibration overestimates the masses by a factor of up to 2 (see Experimental Section), so the real molecular weight could be as low as 150 000 Da. As we do not know the actual correction factor for poly-**6**, we believe it is more appropriate to give a range for M_n, between 150 000 and 300 000 Da. Likewise, the polymerization index N_n spans the range 320−650. The measured polydispersity is close to 3. Similar polydispersities have been measured for other PDAs, e.g., 2.66 for poly-TS12 (TS12 = dodeca-5,7-diyne-1,12-ylene-bis(*p*-toluenesulfonate)[58c] and 2.5 for poly-4BCMU (4BCMU = 5,7-dodecadiyne-1,12-diol bis([(*n*-butoxycarbony1)methyl]urethane)),[59] yet much larger values may be found in some cases. There is no satisfactory explanation for such large polydispersities. Because PDAs are formed by a solid-state topochemical reaction, the usual mass distributions may not apply.

Thus, we have succeeded in preparing an analogue of poly-THD that is soluble in chloroform, a typical solvent for neutral PDAs. Clearly, the presence of two $-CH_2CH_2CH_2-$ fragments in the starting monomer is an asset and greatly improves the solubility of the final polymer. This aspect is of outmost importance for applications requiring the preparation of films.

The fact that poly-**6** is soluble in organic solvents such as chloroform is important for another reason: it allows determination of the polymer contents in more or less polymerized crystals. This is easily accomplished by recording the UV−visible spectrum of the dissolved

(58) See among many references: (a) Patel, G. N.; Chance, R. R.; Witt, J. D. *J. Chem. Phys.* **1979**, *70*, 4387–4392. (b) Plachetta, C.; Rau, N. O.; Hauck, A.; Schulz, R. C. *Makromol. Chem., Rapid Commun.* **1982**, *3*, 249–254. (c) Wenz, G.; Müller, M. A.; Schmidt, M.; Wegner, G. *Macromolecules* **1984**, *17*, 837–850. (d) Aimé, J. P.; Bargain, F.; Fave, J. L.; Rawiso, M.; Schott, M. *J. Chem. Phys.* **1988**, *89*, 6477–6483. (e) Li, Y.; Chu, B. *Macromolecules* **1991**, *24*, 4115–4122.
(59) Rawiso, M.; Aimé, J. P.; Fave, J. L.; Schott, M.; Müller, M. A.; Schmidt, M.; Baumgartl, H.; Wegner, G. *J. Phys.* (*Paris*) **1988**, *49*, 861–880.
(60) Spagnoli, S.; Berréhar, J.; Lapersonne-Meyer, C.; Schott, M.; Rameau, A.; Rawiso, M. *Macromolecules* **1996**, *29*, 5615–5620.
(61) Förster, E. W.; Grellmann, K. H.; Linschitz, H. *J. Am. Chem. Soc.* **1973**, *95*, 3108–3115.

crystal and making use of the extinction coefficient determined previously.

We have measured the absorption dichroism of single crystals of **6** polymerized to very low extents with γ-rays; it is 220 ± 20. From the knowledge of the thickness of the crystals and their polymer contents (see Experimental Section), it is indeed possible to determine the extinction coefficients in perpendicular polarization (the electric field of the incident light being perpendicular to the chain in the crystal), in this case $\alpha_{\perp} = 3300 \pm 200\ cm^{-1}$, and in parallel polarization, $\alpha_{//} = (7.3 \pm 1.1) \times 10^5\ cm^{-1}$. This latter value is similar to that found for other PDAs.[60] Furthermore, such a piece of information allows direct determination of the polymer contents x_p of any studied single crystal without having to dissolve it.

Thermal Reactivity. Diacetylene **6** is almost unreactive thermally. Indeed, a polymer content $x_p \approx 2.6 \times 10^{-7}$ was found after 2.6×10^5 s at 22 °C in the dark, which corresponds to a rate $k_{th} \approx 1 \times 10^{-12}\ s^{-1}$. Similar experiments performed at 45 °C ($k_{th} \approx 6.3 \times 10^{-12}\ s^{-1}$) and 70 °C ($k_{th} \approx 3.5 \times 10^{-11}\ s^{-1}$) yield an activation energy $E_{act} \approx 0.65 \pm 0.05$ eV. These values of $k_i^{(therm)}$ and E_{act} lead to a very small preexponential term, suggesting that the reaction occurs only at particular sites. Then the reaction stops when the sites have all reacted, as is the case for several DAs with hydrogen-bonded side groups, for instance 4BCMU.[62]

This rate may be compared with that of the best studied DA 2,4-hexadiyne-1,6-diol bis(*p*-toluenesulfonate), known in the literature as *p*TS, for which thermal reactivity is intrinsic.[63−68] It is considered as "low" in the initial stages of the reaction (a so-called induction period), then accelerates after a few percents in polymer (poly-*p*TS) are reached. The rate of poly-*p*TS formation in the induction period at 70 °C is $1.7 \times 10^{-6}\ s^{-1}$,[67,68] nearly 5 orders of magnitude larger than the rate of poly-**6** formation. Considering that, in the case of *p*TS, chains formed in the induction period are short (ca. 30 units),[67] while the chains obtained by irradiation of **6** have lengths spanning the range 320−650 units (see above), the ratio of initiation rates between **6** and *p*TS is nearly 1×10^{-6}.

Thermal reactivity of DA crystals and powders has been studied by recording, in a DSC apparatus, the heat evolved during a linear temperature increase.[66,68,69] The very low thermal reactivity of **6** suggests that no significant heat evolution should be detected. Nevertheless, such an experiment was performed and, indeed, no exotherm ascribable to thermal polymerization was observed near 70 °C, below the melting endotherm at 85.5 °C. As a result, thermal polymerization of **6** was not studied further.

UV Polymerization. Two parts of the same crystal were irradiated at 340 and 275 nm respectively, at 20 °C. The diphenylamino (DPA) side groups absorb at both wavelengths whereas the C≡C−C≡C reactive group absorbs only at 275 nm, yet weakly.[70] At 340 nm, the optical density of the crystal was ∼2, so light was almost completely absorbed in the bulk. At 275 nm, the absorption is much larger, so light is totally absorbed in a thin layer near the surface. At that latter wavelength, $\alpha \approx 100\ cm^{-1}$ for the C≡C−C≡C group, so only a small fraction of all photons is absorbed by this group.

The UV reactivity is very low. At 340 nm, $x_p \approx 2.7 \times 10^{-7}$ after 1.45×10^5 s under a photon flux of 1.7×10^{11} photons $cm^{-2}\ s^{-1}$, so the number of monomers included in a polymer chain per absorbed photon is $\eta_p \approx 1.65 \times 10^{-2}$. The same value is found at 275 nm within the experimental uncertainty, ±10%. With a number average polymerization index N_n in the range 320−650, an initiation yield per absorbed photon can be estimated, $2.5 \times 10^{-5} \leq \eta_i = \eta_p/N_n \leq 5 \times 10^{-5}$. This value is nearly 2 orders of magnitude smaller than that found for thoroughly studied *p*TS.[71] η_p varies somewhat among crystals, so it may be that initiation occurs preferentially at defects of unknown nature.

Photoreactivity at 340 nm shows that the reactive C≡C−C≡C groups are excited by energy transfer from the DPA groups. This is allowed by the relative positions of the excited states. The lowest singlet state of DPA groups is at ∼3.85 eV,[72] well below the C≡C−C≡C one at 4.5 eV,[70] so energy transfer cannot occur in the singlet state. But the triplet energies are very close, ∼3.1 eV for DPA groups[73] and ∼3.1 eV for the only C≡C−C≡C fragment where it is known,[74] so there will be a finite probability of populating the C≡C−C≡C triplet at room temperature, by energy transfer in the triplet state following intersystem crossing within the DPA groups. Indeed, the C≡C−C≡C rods are 5−6 Å away from not only the DPA groups of the same molecule, but also from DPA groups of molecules in nearest neighbor stacks (Figure 6). It may be concluded that photopolymerization of **6** is initiated in the diacetylene triplet state, populated by energy transfer from the side group triplet. A detailed study of the phopolymerization of another DA, *p*TS, has led to the conclusion that initiation occurs in the diacetylene triplet state as well.[9]

A similar situation where the side groups absorb at a lower energy than the diacetylene moiety occurs in several other DAs, for instance in DCH (DCH = 1,6-bis(*N*-carbazolyl)-2,4-hexadiyne). Complete polymerization of DCH can be achieved thermally or by γ-irradiation,[75]

(62) Spagnoli, S. Ph.D. Thesis, Université Paris 7, Paris, France, 1995.
(63) Wegner, G. *Makromol. Chem.* **1971**, *145*, 85–94.
(64) Bloor, D.; Koski, L.; Stevens, G. C.; Preston, F. H.; Ando, D. J. *J. Mater. Sci.* **1975**, *10*, 1678–1688.
(65) McGhie, A. R.; Kalyanaraman, P. S.; Garito, A. F. *J. Polym. Sci., Polym. Lett. Ed.* **1978**, *16*, 335–338.
(66) Patel, G. N.; Chance, R. R.; Turi, E. A.; Khanna, Y. P. *J. Am. Chem. Soc.* **1978**, *100*, 6644–6649.
(67) Albouy, P. A.; Keller, P.; Pouget, J. P. *J. Am. Chem. Soc.* **1982**, *104*, 6556–6561.
(68) Bertault, M.; Schott, M.; Brienne, M. J.; Collet, A. *Chem. Phys.* **1984**, *85*, 481–490.
(69) McGhie, A. R.; Lipscomb, G. F.; Garito, A. F.; Desai, K. N.; Kalyanaraman, P. S. *Makromol. Chem.* **1981**, *182*, 965–976.
(70) Berréhar, J.; Lapersonne-Meyer, C.; Schott, M.; Weiser, G. *Chem. Phys.* **2004**, *303*, 129–136.
(71) Schwoerer, M.; Niederwald, H. *Makromol. Chem.* **1985**, No. Suppl. 12, 61–82.
(72) Chakrabarti, S. K. *J. Phys. Chem.* **1971**, *75*, 3576–3580.
(73) Muller, D.; Ewald, M.; Durocher, G. *Can. J. Chem.* **1974**, *52*, 3707–3715.
(74) Bertault, M.; Fave, J. L.; Schott, M. *Chem. Phys. Lett.* **1979**, *62*, 161–165.
(75) Yee, K. C.; Chance, R. R. *J. Polym. Sci., Polym. Phys. Ed.* **1978**, *16*, 431–441.

Table 3. γ-Ray Irradiation Results for Diacetylenes 1−6

compd[a]	γ-ray dose (MRad)	color change	presence of PDA[b]	PDA content (wt %)[b]
1	0.390	no	no	
2	0.590	no	no	
3	0.550	no	no	
4	0.645	no	no	
5	0.645	no	no	
6	0.38	from white	yes	0.35
	0.565	to pale yellow,	yes	0.55
	2	deep orange, or red	yes	2.5
	7	depending on the	yes	5.4
	19.5	irradiation dose	yes	12.5
	25		yes	18.5

[a] The irradiation experiments were carried out on microcrystalline powders (compounds **1**−**5**) or crystals (compound **6**). [b] The presence of PDA was assessed and its amount determined by recording the absorption spectrum of the irradiated material in chloroform solution.

but the UV reactivity of this diacetylene is very low. It has been shown that absorption by the carbazolyl groups can indeed initiate the reaction,[76] yet with very low yield. The comparison between **6** and DCH cannot be pushed too far, however, as the DCH monomer structure is far less favorable to polymerization than that of **6**, and complete γ-polymerization implies a phase transition.[77] Consequently, even the initial γ-reactivity of DCH is low: about 10 MRad are needed to reach a polymer content of about 1.5%.[75,77]

γ-Ray Polymerization. Crystals were irradiated up to a dose of 25 MRad (see Table 3). The polymer content x_p increases linearly with the dose, although the reactivity may be somewhat larger at $x_p < 0.02$. The rate is 7.5×10^{-3} per MRad. So, the number of monomers included in a chain per 100 eV deposited in the crystal, G_p, is about 16, and the number of initiations per 100 eV, $G_i = G_p/N_n$, spans the range $2.5-5 \times 10^{-2}$. This is a low reactivity. For instance, for *p*TS at low doses, G_p is 20 times larger and G_i is around 200 times larger.[66,78] Yet, there are many DAs with reactivities comparable to that of **6**.

The γ-ray reactivity of **6** is much higher than its UV reactivity: the number of initiations per 100 eV (about 20 photons) would be around 1×10^{-3} for UV photopolymerization.

The linear increase in polymer contents as a function of irradiation dose leads to the following conclusions:

(i) Polymerization may be initiated on any monomer and, at the very early stages of the process, an increased contribution of more reactive sites is possible.

(ii) The polymerization conditions do not change at least up to $x_p \approx 0.2$. This observation suggests that N_n and $\eta_i(\gamma)$ remain constant, meaning that the geometrical conditions of initiation and propagation do not change significantly. This is consistent with the similarity that exists between the experimental crystal structure of **6** and the calculated structure (vide infra) of an ordered mixed crystal $(\mathbf{6})_{0.5}-(\text{poly-}\mathbf{6})_{0.5}$.

The large reactivity difference between UV and γ irradiation is reminiscent of 3BCMU.[79] In 3BCMU, this situation was rationalized as being due to a large difference in initiation probabilities between neutral and ionized states. UV irradiation creates only neutral excited states while γ irradiation also creates ionic states (cations and anions). Free charges generated by Compton scattering and subsequent relaxation of the electrons will eventually localize according to the values (in the crystal) of the ionization potentials I_c and electron affinities A_c of the C≡C−C≡C and DPA groups. From the study of charge transfer complexes formed by DPA groups in solution (that is, a condensed phase though liquid), $I_c(\text{DPA}) \approx 7.4$ eV was deduced.[80] The gas phase ionization potential of dimethyldiacetylene is 8.9 eV,[81,82] and I_c has been measured on at least two DA crystals, *p*TS with $I_c = 7.1$ eV,[83] and tricosadiynoic acid[84] with $I_c = 7.0$ eV. These values lead to a polarization correction in the solid of about 1.8 eV, a typical value for this kind of molecular crystal. Thus, positive charges will rather localize on the diacetylene group. It was concluded by Spagnoli et al.[79] that the electron affinity of C≡C−C≡C groups is close to zero. The corresponding value for DPA groups is not available but is likely to be larger. As a result, the electron will rather reside on the side groups, a situation similar to that of 3BCMU and 4BCMU.[79]

In the present case, the reactivity difference can be due either to a difference in initiation rates as in 3BCMU or to the fact that charge transfer to the reactive groups is more efficient than neutral excitation transfer. Thus, γ-ray induced initiation in **6** is likely to be predominantly cationic, the cations being produced by transfer of a charge initially produced elsewhere in the crystal. Note that there has been a thorough study of UV-induced polymerization of *p*TS and, to a lesser extent, of some of its analogues (see the reviews by Sixl[9] and Bässler[78]), but there is no similar work on γ-induced reaction.

Spectroscopic Studies of Partially Polymerized Single Crystals. The Raman, absorption and luminescence studies presented here were performed on two separate single crystals of **6** irradiated with different doses of γ-rays, 0.38 MRad for crystal C1 ($x_p = 3 \times 10^{-3}$) and 4500 Rad for crystal C2 ($x_p \approx 3 \times 10^{-5}$).

Raman studies were conducted at various temperatures on the most irradiated crystal C1 as this crystal gives a better signal-to-noise ratio. The Raman spectrum of crystal C1 was measured at 15 K (Figure 8) to allow direct comparison with the vibration mode frequencies calculated at 0 K (see computational results, below). At 15 K, the experimental stretching frequencies of the double bond (ν_D) and the triple bond (ν_T) for the conjugated system in

(76) Chance, R. R.; Baughman, R. H. *8th Molecular Crystal Symposium, Book of Abstracts*; Santa Barbara, CA, May 29−June 2, 1977; p 47.
(77) Enkelmann, V.; Leyrer, R. J.; Schleier, G.; Wegner, G. *J. Mater. Sci.* **1980**, *15*, 168–176.
(78) Bässler, H. *Adv. Polym. Sci.* **1984**, *63*, 1–48.
(79) Schott, M.; Spagnoli, S.; Weiser, G. *Chem. Phys.* **2007**, *333*, 246–253.
(80) Briegleb, G.; Czekalla, J. *Z. Elektrochem. Angew. Phys. Chem.* **1959**, *63*, 6–12.
(81) Brogli, F.; Heilbronner, E.; Hornung, V.; Kloster-Jensen, E. *Helv. Chim. Acta* **1973**, *56*, 2171–2178.
(82) Rao, C. N. R.; Basu, P. K.; Hegde, M. S. *Appl. Spectrosc. Rev.* **1979**, *15*, 1–193.
(83) Murashov, A. A.; Silinsh, E. A.; Bässler, H. *Chem. Phys. Lett.* **1982**, *93*, 148–150.
(84) Seki, K.; Morisada, I.; Edamatsu, K.; Tanaka, H.; Yanagi, H.; Yokoyama, T.; Ohta, T. *Phys. Scr.* **1990**, *41*, 172–176.

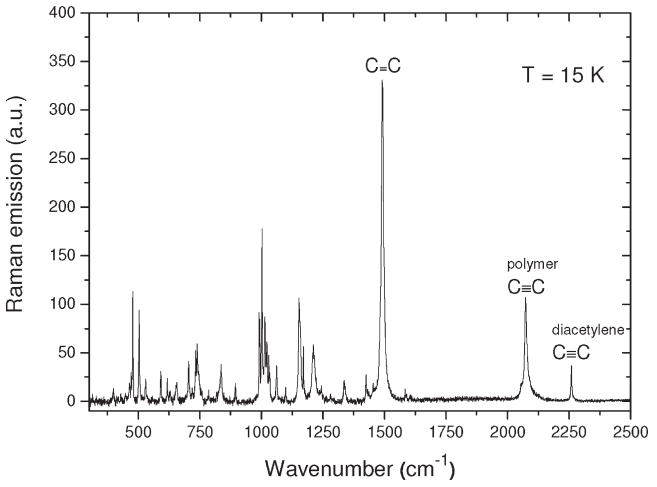

Figure 8. Raman spectrum of crystal C1 at 15 K. The excitation wavelength was 647 nm. The polymer line intensities are enhanced by strong preresonance. The double bond and triple bond stretching mode frequencies are respectively 1491 ± 2 and 2073 ± 2 cm^{-1} at 15 K. The diacetylene triple bond stretching mode frequency is 2259 ± 2 cm^{-1}. The spectrum is not corrected for detection response.

the ground state are 1491 ± 2 cm^{-1} and 2073 ± 2 cm^{-1}, respectively. The frequency of the Raman-active monomer triple bond stretching mode is 2259 ± 2 cm^{-1}, which is typical. Figure 8 also shows modes at lower frequencies that will not be discussed here. In addition, plots of ν_D and ν_T versus temperature between 15 and 300 K (not shown) are smooth, which indicates that no phase transition occurs as temperature is changed.[85,86]

Figure 9 shows the absorption and luminescence spectra of crystal C2 at 13 K for a polarization of the excitation parallel to the chains. The direction of the chains is along the length of the crystal; this can be easily verified by taking advantage of the high dichroism of the crystal. Despite a blue shift of the bands as compared to those of all other PDA crystals, the overall structures of the absorption and luminescence spectra are typical of polydiacetylenes, i.e., they show a main zero-phonon excitonic line accompanied by weaker vibronic replicas. The spectra shown in Figure 9 are well-resolved, and the luminescence spectrum is nearly a mirror image of the absorption spectrum. The lines are broadened at higher temperatures.

The zero-phonon emission line width at 13 K might be affected by reabsorption. The position (~2.4 eV) of the unperturbed emission line at this temperature can be recovered by using the frequencies of the double bond and triple bond stretching modes determined by Raman spectroscopy (see Figure 8). In these conditions, a Stokes shift less than ~2 meV is estimated, the latter being possibly zero. A detailed investigation of the spectroscopic properties of poly-**6** will be presented elsewhere.[87]

In conclusion, the polymeric chains generated by γ-ray irradiation of single crystals of **6** are highly luminescent. The similarity between the spectroscopic features of these chains and those of isolated red chains of poly-3BCMU, known to be perfect quasi-1D quantum wires,[27,28] suggests that the former chains also have a high degree of order. The spectroscopic properties of poly-**6** chains compare well with those of poly-THD chains which are strongly luminescent at low temperature,[33,37] the structural difference between their monomers being two methylene groups per half-molecule. Given that **6** is much less reactive than THD, the amount of polymer produced by irradiation of single crystals of the former diacetylene can be easily controlled. This is a quite remarkable result, as it allows spectroscopic investigation of polydiacetylenes in a large range of conditions and makes possible the study of the relationship that exists between chain conformation and electronic properties. As far as the origin of the blue shift mentioned earlier is concerned, the X-ray crystal structure of **6** suggests that it might be connected with the unusual configuration of the polymer chains (vide infra).

Computational Studies of 6 and Poly-6. The high thermal reactivity of THD allows the preparation of totally polymerized poly-THD crystals of high enough quality to allow structural determination of this polymer with high accuracy.[32] This is not the case for **6** because of its low reactivity. To circumvent this difficulty, we have used DFT methods to obtain the structure of poly-**6**. Prior to doing that, however, we have assessed the accuracy of our computational method by comparing the calculated structure of monomer **6** with the experimental one.

Semilocal DFT-GGA methods like PBE are certainly among the most efficient computational methods in condensed matter, but their drawback is that they do not include the London dispersion part of the weak van der Waals interactions.[88] As a result, in molecular crystals, covalent bonds are well-reproduced, whereas intermolecular distances and lattice parameters are overestimated. If London forces are the dominant interactions, as is the case in a noble gas crystal, this leads to unrealistic structures; but in a molecular crystal, where other contributions dominate, GGA-DFT can give fairly good structures. We have checked this effect on our calculations by optimizing the atomic positions and unit cell parameters of diacetylene **6**, starting from the experimental values. The computed fully optimized (atomic positions and unit cell) structure is still close to the experimental one with an expansion of the lattice parameters by 5% (Table 4). This expansion is reasonable for a DFT calculation, suggesting that the contribution of dispersion forces to intermolecular forces is moderate, and that dipole−dipole van der Waals interactions dominate. Intramolecular distances are all within the typical error of the method, that is around 2%. The theoretically determined bond lengths agree well with the values found for diacetylenes for which an X-ray crystal structure has been reported.[3]

(85) Batchelder, D. N.; Bloor, D. *Adv. Infrared Raman Spectrosc.* **1984**, *11*, 133–209.
(86) Spagnoli, S.; Berrehar, J.; Fave, J.-L.; Schott, M. *Chem. Phys.* **2007**, *333*, 254–264.
(87) Al Choueiry, A.; Barisien, T.; Holcman, J.; Legrand, L.; Schott, M.; Weiser, G.; Balog, M.; Deschamps, J.; Dutremez, S. G.; Filhol, J.-S. *Phys. Rev. B* **2010**, *81*, 125208−1–125208−11.
(88) Kohn, W.; Meir, Y.; Makarov, D. E. *Phys. Rev. Lett.* **1998**, *80*, 4153–4156.

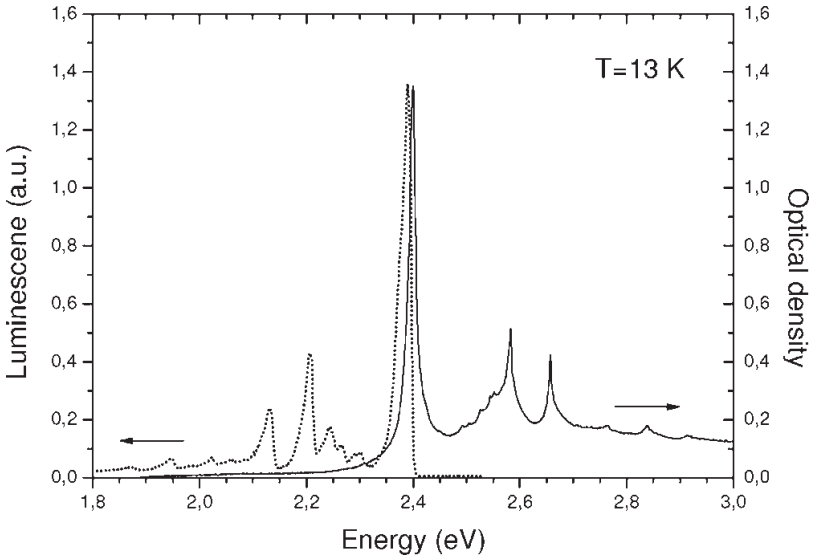

Figure 9. Absorption (solid line) and luminescence (dots) spectra of crystal C2 at $T = 13$ K for a polarization of the excitation parallel to the polymer chains. For the luminescence measurements, the excitation was 2 mW at 488 nm.

Table 4. Comparison Between Calculated and Experimental Parameters for 6 and Poly-6[a,b]

compd	lattice params (distances in Å and angles in deg)	torsion angle θ (deg)	energy/unit cell (kJ mol^{-1})	C≡C length (Å)	C=C length (Å)	C−C length (Å)	R_v[c] (Å)	d[c] (Å)
6 as calculated in optimized unit cell	$a = 10.48$, $\alpha = 90.00$, $b = 16.88$, $\beta = 97.01$, $c = 17.41$, $\gamma = 90.00$		0	1.224		1.360, 1.452, 1.453, 1.537−1.543	3.764, 3.804	5.164, 5.543
6 as calculated in exp unit cell	$a = 9.948$, $\alpha = 90.0$, $b = 16.089$, $\beta = 98.697$, $c = 16.764$, $\gamma = 90.0$		110.7	1.224		1.358, 1.449, 1.449, 1.533−1.540	3.503, 3.541	4.906, 5.349
6 exp	$a = 9.948$, $\alpha = 90.0$, $b = 16.089$, $\beta = 98.697$, $c = 16.764$, $\gamma = 90.0$			1.194, 1.196		1.379, 1.461, 1.464, 1.5217−1.5240	3.4946, 3.573	4.937, 5.281
poly-**6** as calculated in optimized unit cell	$a = 9.97$, $\alpha = 83.86$, $b = 17.59$, $\beta = 95.98$, $c = 17.44$, $\gamma = 89.37$	119	−230.0	1.236	1.387	1.430		
poly-**6** as calculated in the unit cell of **6**	$a = 9.948$, $\alpha = 90.0$, $b = 16.089$, $\beta = 98.697$, $c = 16.764$, $\gamma = 90.0$	136	−104.5	1.239	1.393	1.427		

[a] The torsion angle θ is depicted in Figure 10 and is equivalent to the R−$C_4\cdots C_1$−R dihedral angle in Scheme 1. [b] Energies are relative to that of the monomer in the optimized cell. [c] See Scheme 1.

We have also obtained the optimized structure of **6** in the experimental unit cell: intermolecular and intramolecular distances are within 2% of the experimental ones. This structure is only 0.5 kJ mol^{-1} per atom less stable than the fully relaxed one, suggesting that the very weak forces missing in the calculation are not important for our purpose. In both cases, the unit cell size does not have much effect on vibration frequency calculation results as the typical error is a systematic overestimation by only 1−1.2% (Table 5). The computed symmetric C≡C stretching frequency of **6** is 2276 cm^{-1} in the relaxed unit cell and 2286 cm^{-1} in the experimental unit cell, in good agreement with the experimental value of 2259 cm^{-1} at 15 K. Aromatic C=C vibrations for **6** are computed to be in the following ranges: 1555−1558, 1570−1572, 1576−1583, and 1591−1595 cm^{-1} (optimized unit cell), and 1563−1568, 1575−1576, 1581−1590, and 1600−1604 cm^{-1} (experimental unit cell). The corresponding vibrations in the experimental spectrum are 1573, 1592, and 1604 cm^{-1}.

Our ground state calculations appear to reproduce well the structure and properties of **6**. On the basis of these findings, we expect the computed structure of poly-**6** to be a faithful model of actual poly-**6** with properties directly comparable with the experimental results.

Poly-**6** was generated computationally bearing in mind the experimental situation, that is a monomer-polymer mixed crystal in which polymer chains are surrounded by monomer molecules. As the computational method requires a 3D periodic system and a not too large unit cell because of computational cost, an ordered $(\text{monomer})_{0.5}$−$(\text{polymer})_{0.5}$ mixed crystal was considered: one out of the two monomer stacks in the unit cell was replaced by a polymer chain. In this situation, a polymer chain is surrounded by side groups from nearest neighbor diacetylene stacks. The polymeric structure was built by rotation of the monomer units until the distance between the carbon atoms that get connected during the polymerization process was 1.51 Å, a distance reasonably

Table 5. Comparison Between Calculated and Experimental Properties of 6 and Poly-6

compound	C≡C vibration (cm^{-1})	aromatic C=C vibration (cm^{-1})	enyne C=C vibration (cm^{-1})	DFT gap (eV)	color
6 as calculated in optimized unit cell	2276	1555−1558, 1570−1572, 1576−1583, 1591−1595		2.91	
6 as calculated in exp unit cell	2286	1563−1568, 1575−1576, 1581−1590, 1600−1604		2.83	
6 exp at T = 300 K	2256[a]	1573, 1592, 1604			
poly-**6** as calculated in optimized unit cell	2075		1471, 1512	1.65	red
poly-**6** as calculated in the unit cell of **6**	2076		1458, 1494	1.32	red
poly-**6** exp at T = 300 K	2045[b]		1480[c]		red

[a] C≡C vibration at 15 K = 2259 cm^{-1}. [b] C≡C vibration at 15 K = 2073 cm^{-1}. [c] Enyne C=C vibration at 15 K = 1491 cm^{-1}.

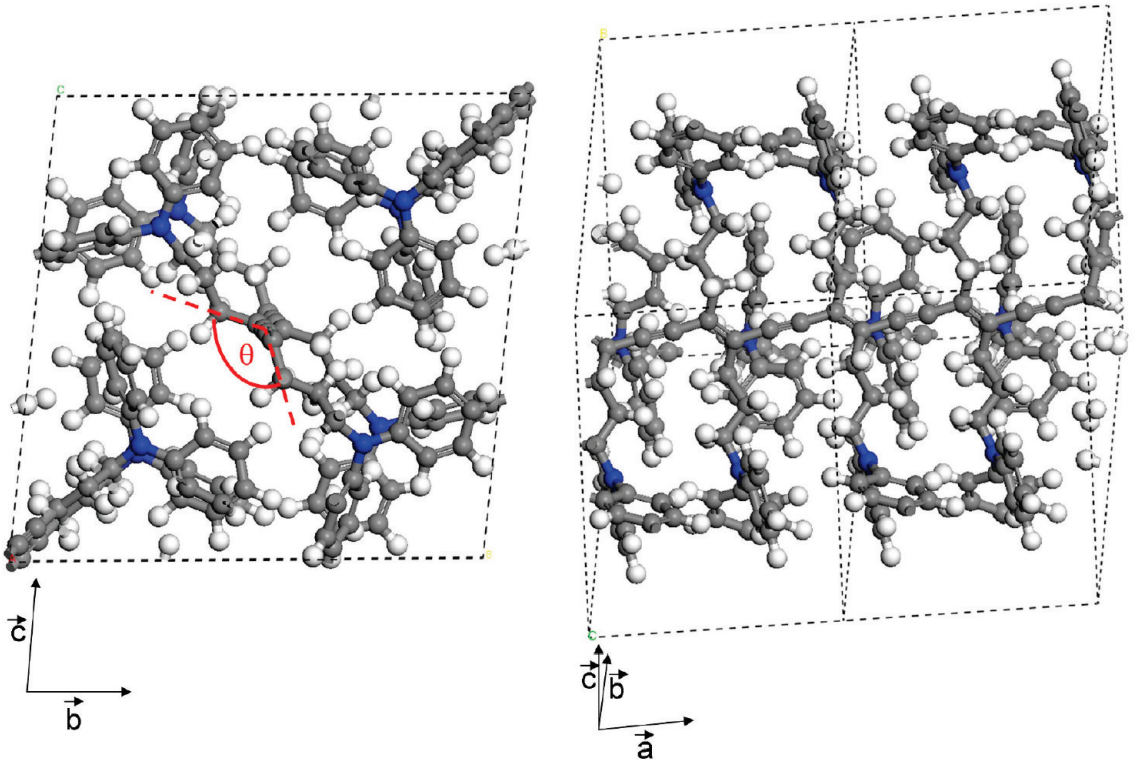

Figure 10. Structure of partially polymerized **6** as obtained from calculations using a fully relaxed cell. The torsion angle θ of the chain is shown in the picture on the left-hand side.

close to the C=C bond length of a PDA chain. Then, the atomic positions and unit-cell parameters were optimized.

By analogy with the situation found in *p*TS-poly-*p*TS mixed crystals,[89,90] the optimized unit cell at 50% polymer contents should be close to that of the pure polymer, whereas optimization in the monomer experimental cell should mimic the situation of an isolated poly-**6** chain in its monomer crystal, giving some insight into the strain of the chain in that situation. Hence, poly-**6** was computed in a fully relaxed unit cell and in the experimental cell of monomer **6** as shown in Figure 10.

Formation of poly-**6** is calculated to be exothermic by 108 (kJ mol^{-1})/unit cell in the experimental cell as opposed to 115 (kJ mol^{-1})/unit cell in the optimized cell. This polymerization energy is smaller than that found for other polydiacetylenes such as poly-THD (135 kJ mol^{-1} per monomer),[39] poly-*p*TS (155 kJ mol^{-1} per monomer),[66,68,91] and poly-[1,6-bis(2,4-dinitrophenoxy)-2,4-hexadiyne] (135 kJ mol^{-1} per monomer), known as poly-DNP.[69]

(89) Aimé, J.-P. Ph.D. Thesis, Université Paris 7, Paris, France, 1984.
(90) Bloor, D.; Day, R. J.; Ando, D. J.; Motevalli, M. *Brit. Polym. J.* **1985**, *17*, 287–293.
(91) Chance, R. R.; Patel, G. N.; Turi, E. A.; Khanna, Y. P. *J. Am. Chem. Soc.* **1978**, *100*, 1307–1309.

For the fully optimized structure, the calculated unit cell volume decreases slightly from 3058 Å^3 to 3025 Å^3 upon polymerization; the decrease in the *a* cell parameter due to formation of carbon−carbon bonds is compensated by an increase in the *b* parameter. Packing of the phenyl groups is not much affected by these changes and is mostly conserved, even though some strain appears.

Most important is the fact that the polymeric chain is not planar but is strongly twisted with a torsion angle θ, shown in Figure 10 and equivalent to the R−C$_4$···C$_1$−R dihedral angle in Scheme 1, of 136° (it is 119° in the optimized cell). In a recent study,[39] we have shown that such a twisted structure can be associated with a red phase PDA. The bond lengths of the polymer backbone (Table 4) are consistent with those computed previously for poly-THD[39] and poly-[(1,6-bis-(*N*-methylimidazolium)-2,4-hexadiyne)dibromide].[92]

The full vibration spectrum of poly-**6** was next calculated, as comparison between computed and experimental frequencies can provide some information about local geometries.[93,94] As opposed to typical planar PDAs, for twisted PDA chains like poly-**6** described herein and poly-THD,[39] two vibrational frequencies associated with the C=C stretches are possibly Raman active. Calculations using a relaxed unit cell yield a symmetric C≡C stretching frequency of 2075 cm^{-1} and C=C stretching frequencies of 1471 and 1512 cm^{-1} (Table 5). For poly-**6** optimized in the unit cell of **6**, a symmetric C≡C stretching frequency is found at 2076 cm^{-1}, and C=C stretching frequencies are found at 1458 and 1494 cm^{-1}. The relative intensities of the corresponding Raman peaks cannot be easily computed at this level of theory because of the size of the system. However, taking into account the accuracy of the computational method, these stretching frequencies are equal to the experimental ones at 15 K (2073 and 1491 cm^{-1}, respectively). Such a good agreement is a clear indication that the calculated structure of poly-**6** should be very close to the experimental one and lends strong support to the former being a good model of the latter.

Usually, blue phase PDAs have C≡C stretching frequencies around 2080 cm^{-1} and C=C stretching frequencies around 1460 cm^{-1}. Red phase PDAs have C≡C stretching frequencies around 2120 cm^{-1} and C=C stretching frequencies around 1520 cm^{-1}. The measured C≡C stretching frequency of poly-**6** is suggestive of a blue phase PDA, and the experimentally observed C=C stretching frequency is at the boundary between a blue phase and a red phase (Table 5). Yet, the fact that poly-**6** is strongly luminescent is a clear indication that it is a red phase PDA;[34,37] a similar dilemma between blue phase and red phase PDAs has been encountered previously in the case of poly-THD.[39]

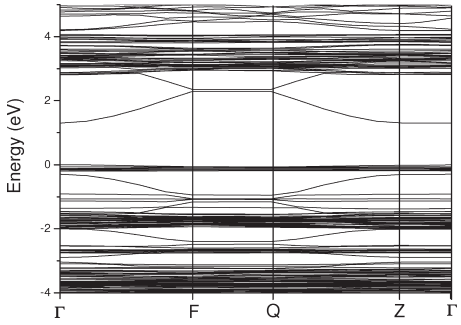

Figure 11. Band structure of partially polymerized **6** in the monomer unit cell. The relative coordinates of the given *k*-points are: Γ(0,0,0), F(0.5,0,0), Q(0.5,0.5,0), and Z(0,0.5,0). Fermi level is at 0 eV.

Clearly, the correlation between optical absorption and luminescence on the one hand, and ground state vibrational frequencies (as obtained from resonant Raman scattering for instance) on the other hand, may not be as unequivocal as previously assumed. The question concerning the variation of vibrational frequencies of PDAs in relation to color changes will be further discussed elsewhere.[95] Let us only point out here that elastic strain of a PDA chain may result in large variations of both the absorption threshold and vibrational frequencies; this has been well studied in poly-*p*TS for instance. Frequency changes may be related to anharmonicity, or indirectly to the effect of strain on the electronic structure. Most experimental studies used longitudinal tensile strain, but compressive strain also leads to large effects, of the opposite sign.[86] Such effects may be at play in poly-**6** but hardly so in poly-THD.

We computed recently a model PDA with an unstrained structure, poly-2,4-hexadiyne, that can be used as a reference.[39] The lack of any local structural stress in this PDA is due to the absence of inter- and intrachain interactions in the large chosen unit cell. We find that the C−C, C=C, and C≡C bonds of poly-**6** (Table 4) are all longer by more than 0.01 Å than those of the unstressed model chain with the same torsion angle of 119°, i.e., d(C−C) = 1.416 Å, d(C=C) = 1.378 Å, and d(C≡C) = 1.228 Å. Such an observation suggests that the main chain of poly-**6** is under tensile stress. The strain is linked to the presence of bulky substituents that govern crystal packing. In a Morse potential approach, all of the carbon−carbon bonds of poly-**6** are expected to be weakened due to anharmonicity, and associated frequencies should be shifted toward lower values as compared to those of the unstressed model (ν_T = 2142 cm^{-1} and ν_D = 1519 cm^{-1}).[39] Our calculations agree with this reasoning. In addition, C≡C bonds appear to be much more sensitive to local stress than C=C bonds, certainly because of a larger bond anharmonicity. This leads to a shift of the red poly-**6** frequencies toward values typically observed for blue isomers, and to a large temperature dependence. Clearly, for some PDAs, the interplay between the twisting of the polymer chain and the strain in this chain can lead to C≡C and C=C Raman frequencies outside typical ranges.

The electronic band structure of half-polymerized **6** in the monomer unit cell was computed and is presented

(92) Chougrani, K.; Deschamps, J.; Dutremez, S.; van der Lee, A.; Barisien, T.; Legrand, L.; Schott, M.; Filhol, J.-S.; Boury, B. *Macromol. Rapid Commun.* **2008**, *29*, 580–586.
(93) Filhol, J.-S.; Simon, D.; Sautet, P. *J. Phys. Chem. B* **2003**, *107*, 1604–1615.
(94) Ben Yahia, M.; Lemoigno, F.; Beuvier, T.; Filhol, J.-S.; Richard-Plouet, M.; Brohan, L.; Doublet, M.-L. *J. Chem. Phys.* **2009**, *130*, 204501−1–204501−11.
(95) Filhol, J.-S., work in progress.

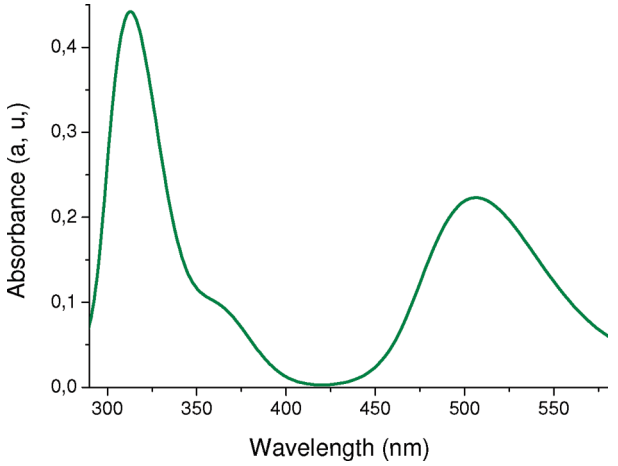

Figure 12. Calculated absorption spectrum of partially polymerized **6** in the unit cell of the monomer.

in Figure 11. It corresponds to a direct band gap semiconductor at Γ-point with a DFT gap of 1.32 eV. The lowest strongly dispersed unoccupied band corresponds to the π^* system of the polymer; the eight highest occupied bands, that do not exhibit much dispersion, correspond to the nitrogen lone pairs of the amino groups. The next highest band corresponding to the polymer π system is located 0.27 eV below Fermi level. Thus, the peculiarity of this polymer is to have intermediate nitrogen bands inserted between the $\pi-\pi^*$ band structure, similarly to what was found for poly-THD.[39]

The absorption spectrum of poly-**6** in the experimental unit cell is presented in Figure 12; this spectrum was computed using a scissor operator of 0.65 eV and a smearing factor of 0.15 eV. It shows two large absorption bands centered at about 312 and 505 nm. The first band is linked to the NPh_2 moiety and the second band to the enyne backbone of the polymer. Considering the 505 nm absorption, poly-**6** is expected to be a red phase PDA.[17] The calculated absorption maximum is only 10 nm lower than the experimental value in the crystal, i.e., 515 nm (see Figure 9).

In summary, the structure of poly-**6** was computed and some of its properties calculated. Agreement between calculated and experimental values is quite good. Poly-**6** is a red phase PDA with a 136° twisted enyne backbone that absorbs in the blue part of the visible spectrum. Its Raman C≡C and C=C stretching frequencies are shifted toward blue values because of tensile strain.

Relationship between Spectroscopy and Structure of Poly-6. The transition energy of the exciton for poly-THD, as deduced from electroreflectance measurements, is 2.171 eV at 16 K.[37] Such a value is typical of red PDAs, that is around 2.2 eV. For poly-**6**, the transition energy of the exciton, as determined from absorption and luminescence studies (vide supra), is about 2.4 eV. Thus, poly-**6** absorbs at a much higher energy than poly-THD. It was suggested in a recent computational study that the difference in exciton energies between blue and red phase PDAs was due to conformational differences in the polymer chains, blue chains being flat (the $R-C_1\cdots C_4-R$ dihedral angle in Scheme 1 being equal to 180°), and red chains being twisted (the $R-C_1\cdots C_4-R$ dihedral angle in Scheme 1 being different from 180°).[39] It was also put forth that the transition energy of the exciton is an intrinsic property of the chain and that the electronic nature of the substituents only have a modest influence on it. Yet, distortion of the chains as a result of crystal packing forces, to which the size of the substituents and the presence of interactions with neighboring groups both contribute largely, is of outmost importance. Hence, for red PDAs, a multitude of conformational isomers is possible depending on the nature of the substituents.

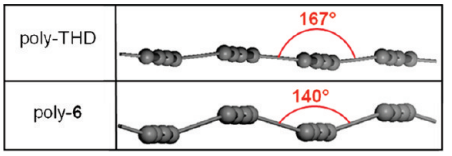

Figure 13. Comparison between the undulation found in poly-THD chains and that found in poly-**6** chains.

With this in mind, the fact that poly-**6** absorbs higher energy photons than poly-THD suggests that the former polymer has a more twisted structure than the latter. We have found that it is indeed the case: the $C_1{=}C_4\cdots C_1{=}C_4$ dihedral angle (see Scheme 1) is 167° in poly-THD and 140° in poly-**6** (Figure 13). These angles match closely the $R-C_4\cdots C_1-R$ dihedral angles, 166° for poly-THD[32] and 136° for poly-**6** optimized in the unit cell of the monomer (Table 4).

The X-ray crystal structure of the monomer THD is not known, so it is not possible to say to which extent the wavy shape of the conjugated backbone resembles the structure of the starting monomer. But the structure of **6** is known; in this case, the $C_4\cdots C_1\cdots C_4\cdots C_1$ dihedral angle formed by three reacting monomers (see Scheme 1) is 140°, in excellent agreement with that found in the polymer. This result was somewhat expected based on the fact that diacetylene polymerization abides by the topochemical concept (i.e., the reaction proceeds under minimal atomic and molecular displacement). However, larger differences are observed in the positions of the substituents between the monomer and the polymer.

Conclusions

Several analogues of 1,6-bis(diphenylamino)-2,4-hexadiyne (THD) have been synthesized and their solid-state structures determined by single-crystal X-ray diffraction. It was found that a modification of the aromatic rings (substitution of one or several phenyl hydrogens by methyl or fluorine groups), or the introduction of methylene spacers between the nitrogen atoms and the phenyl rings, led to an A-A-A-A arrangement of the diacetylenic molecules in the unit cell. Such an arrangement is unfavorable to polymerization of the C≡C−C≡C moieties because these moieties lie too far apart from each other along the polymerization axis. On the other hand, replacement of the methylene groups of THD by longer spacers, $(CH_2)_4$ in the case of **5** and $(CH_2)_3$ in the case of **6**, yields an A−B−A−B structural arrangement of the diacetylenic molecules. Such an arrangement is probably

also present in THD but, since the X-ray crystal structure of this compound is not known, this is not certain. Diacetylene **5** does not polymerize in the solid state while **6** does, and this result agrees with the fact that **6** matches Baughman's criteria for topochemical polymerization and **5** does not. The thermal solid-state polymerization reactivity of **6** is low as well as its UV polymerization reactivity, but its γ-ray polymerization reactivity is much higher, suggesting that γ-ray induced initiation in **6** may be predominantly cationic. Nonetheless, the solid-state polymerization reactivity of **6** is much lower than that of THD, thereby validating our working hypothesis that modulation of the polymerization reactivity of THD analogues via a molecular engineering approach should be possible. Similar efforts have been made in the past with *p*TS derivatives and BCMU analogues.

Poly-**6** is soluble in organic solvents such as chloroform and THF, so we were able to determine its molecular weight by SEC, between 150 000 and 300 000 Da. The polymeric chains generated by γ-ray irradiation of single crystals of **6** are highly luminescent, which signifies that poly-**6** is a red phase PDA just like poly-THD. In addition, the similarity between the spectroscopic features of poly-**6** chains and those of isolated red chains of poly-3BCMU, known to be perfect quasi-1D quantum wires,[27,28] suggests that the former chains also have a high degree of order.

The structure of poly-**6** in its monomer matrix was obtained by DFT calculations. As anticipated from the strong luminescence, it was found that poly-**6** chains are considerably twisted with a $C_1{=}C_4\cdots C_1{=}C_4$ dihedral angle of 140°. This angle is comparable to that found in the starting monomer, 140°, suggesting that the arrangement of the monomer molecules in the crystal lattice has a decisive influence on the shape of the resulting polymeric chain.

The transition energy of the exciton for poly-**6**, about 2.4 eV, is much higher than that of poly-THD, 2.171 eV at 16 K. On the basis of previous theoretical work on the colors of PDAs,[39] this difference was expected to be due to dissimilarities in the $C_1{=}C_4\cdots C_1{=}C_4$ dihedral angle between the two polymers. We have found that this is true: the $C_1{=}C_4\cdots C_1{=}C_4$ dihedral angle is 167° in poly-THD and 140° in poly-**6**.

Hence, poly-**6** is a new structural type of PDAs and turns out to be a good model for the study of the relationship that exists between chain conformation and electronic structure. Work is currently ongoing to characterize further poly-**6** and, in particular, study the variation of its photophysical properties as a function of polymer contents. Also, the preparation of an analogue of **6** with ethylene groups between the diacetylene fragment and the NPh_2 moieties instead of propylene groups will begin in due course.

Experimental Section

Spectroscopic and Characterization Methods. Solution ^{1}H and ^{13}C NMR spectra were obtained on a Bruker AVANCE DPX 200 instrument. ^{1}H chemical shifts were referenced to the protio impurity of the NMR solvent and ^{13}C chemical shifts to the NMR solvent. ^{19}F NMR spectra were recorded on a Bruker AC 250 or an AVANCE 300 spectrometer and were referenced to $CFCl_3$. Infrared spectra were recorded on a Thermo Nicolet Avatar 320 FT-IR spectrometer with a 4 cm^{-1} resolution. Absorption spectra of solutions and crystals were measured in the double beam mode on a Cary 5000 double monochromator. Raman spectra of powdered samples were obtained at room temperature on a Bruker RFS100 FT spectrometer equipped with a continuous YAG laser (λ = 1064 nm) as a light source and a germanium detector. Single-crystal Raman and luminescence measurements were performed with a Jobin Yvon Ramanor U1000 double monochromator. Excitation used argon or krypton laser lines. For variable-temperature (10−300 K) solid-state absorption, Raman, and luminescence studies, a helium gas exchange cryostat was utilized. FAB mass spectra were obtained on a Jeol JMS-SX102A instrument and ESI mass spectra on a Micromass QTOF spectrometer. Melting points were measured on a Büchi B-540 melting point apparatus and are uncorrected. C, H, N elemental analyses were performed in-house using a Thermo Finnigan FLASH EA 1112 Series analyzer.

Materials. The chemicals used in this study were obtained from the following commercial sources: diphenylamine (Aldrich), dibenzylamine (Avocado), di-*p*-tolylamine (Aldrich), 80 wt % solution of propargyl bromide in toluene (Acrōs Organics), 18-crown-6 (Acrōs Organics), 5-hexyn-1-ol (Alfa Aesar), 4-pentyn-1-ol (Alfa Aesar), *p*-toluenesulfonyl chloride (Avocado), triethylamine (Riedel-de Haën), 2.5 M solution of *n*-butyllithium in hexanes (Aldrich), copper(I) chloride (Aldrich), TMEDA (Lancaster), potassium hydroxide (Prolabo), potassium carbonate (Prolabo). Solvents were purchased from the following suppliers: THF (Prolabo), DMF (Acrōs Organics), methanol (Prolabo), DME (Aldrich), ethyl acetate (Carlo Erba). Bis(pentafluorophenyl)amine and (*N*-pentafluorophenyl)phenylamine were synthesized following reported methods.[45,46]

General Considerations. All of the syntheses involving air-sensitive materials were carried out under an inert atmosphere of argon using standard Schlenk-line techniques. Prior to use, THF was distilled over sodium-benzophenone ketyl, and triethylamine and TMEDA were distilled over calcium hydride. Diphenylamine was purified by sublimation.

Syntheses of (*N*-Pentafluorophenyl)(*N*-phenyl)propargylamine (7), *N*,*N*-Bis(*p*-tolyl)propargylamine (8), Dibenzylpropargylamine (9), *N*,*N*-Bis(pentafluorophenyl)propargylamine (10), 5-Hexynyldiphenylamine (11), 4-Pentynyldiphenylamine (12), 5-Hexyn-1-*p*-toluenesulfonate (13), and 4-Pentyn-1-*p*-toluenesulfonate (14). See the Supporting Information.

Synthesis of 1,6-Bis((*N*-pentafluorophenyl)phenylamino)-2,4-hexadiyne (4). A mixture of CuCl (16.8 mg, 0.17 mmol), TMEDA (0.31 mL), and methanol (20 mL) was prepared and stirred for 30 min, after which time air was bubbled into it for 1 h. Alkyne **7** (0.5 g, 1.7 mmol) was added and the mixture was stirred vigorously at room temperature for 24 h with continuous air bubbling. A precipitate formed during the reaction. The suspension was concentrated to dryness and the residue washed with three 10 mL portions of methanol. The resulting solid was dissolved in dichloromethane (30 mL). The dichloromethane solution was washed with three 10 mL portions of deionized water and dried over magnesium sulfate, and the solvent was evaporated off. The residue was purified by column chromatography on silica gel with use of a 90:10 v/v mixture of *n*-pentane and diethyl ether as eluent. A white solid was obtained (0.35 g, 70%). Mp 85.3 °C. ^{1}H NMR (200.1 MHz, $CDCl_3$): δ 4.43 (s, 4H; H3), 6.79 (d, 4H; H9), 6.94−7.02 (m, 2H; H11),

7.26−7.36 (m, 4H; H10). ^{19}F NMR (282.4 MHz, $CDCl_3$): δ −161.6 (m, 4F; F6), −156.2 (t, $^3J_{FF}$ = 21.6 Hz, 2F; F7), −144.1 (m, 4F; F5). ^{13}C NMR (50.3 MHz, $CDCl_3$): δ 42.3 (C3), 69.6 (C1), 74.2 (C2), 114.9 (C9), 120.4 (m; C4), 121.3 (C11), 129.8 (C10), 138.8 (dm, $^1J_{CF}$ = 251 Hz; C7), 140.8 (dm, $^1J_{CF}$ = 255 Hz; C6), 146.0 (C8), 146.0 (dm, $^1J_{CF}$ = 255 Hz; C5). Raman (neat powder): $\tilde{\nu}$ 2256, 1654, 1602 cm^{-1}. FAB+ MS (NOBA) *m*/*z* (%): 592 (40) $[M]^+$, 334 (58) $[M-N(C_6H_5)(C_6F_5)]^+$. Elemental anal. Calcd (%) for $C_{30}H_{14}F_{10}N_2$ (592.43): C, 60.82; H, 2.38; N, 4.73. Found: C, 60.61; H, 3.35; N, 4.37.

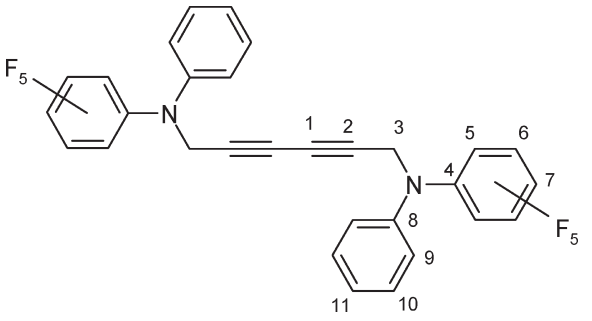

Synthesis of 1,6-Bis(di-*p*-tolylamino)-2,4-hexadiyne (2). The same protocol as that leading to **4** was followed except that **7** was replaced with **8** (0.70 g, 3.0 mmol). In this case, a large amount of precipitate formed after air bubbling for 30 h that was then filtered on a glass frit and washed with methanol. The solid was dissolved in dichloromethane. The dichloromethane solution was washed three times with deionized water and dried over magnesium sulfate, and the solvent was evaporated off. A white solid was obtained (0.42 g, 60%). Mp 172.2 °C. ^{1}H NMR (200.1 MHz, $CDCl_3$): δ 2.34 (s, 12H; H8), 4.42 (s, 4H; H3), 6.92−6.99 (m, 8H; H5), 7.10−7.14 (m, 8H; H6). ^{13}C NMR (50.3 MHz, $CDCl_3$): δ 21.1 (C8), 43.3 (C3), 69.0 (C1), 75.3 (C2), 121.6 (C5), 130.3 (C6), 132.0 (C7), 145.5 (C4). Raman (neat powder): $\tilde{\nu}$ 3065, 2919, 2254, 1613, 807 cm^{-1}. FAB+ MS (NOBA) *m*/*z* (%): 468 (23) $[M]^+$, 210 (29) $[(C_7H_7)_2NCH_2]^+$, 91 (20) $[C_7H_7]^+$. Elemental anal. Calcd (%) for $C_{34}H_{32}N_2$ (468.63): C, 87.14; H, 6.88; N, 5.98. Found: C, 85.68; H, 7.71; N, 5.80.

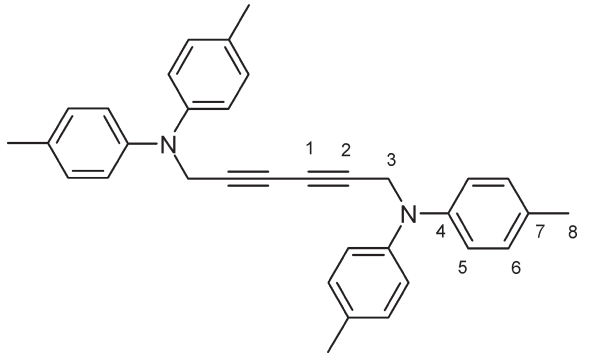

Synthesis of 1,6-Bis(dibenzylamino)-2,4-hexadiyne (1). Diyne **1** was prepared similarly to **2** by using **9** (4.65 g, 19.8 mmol) instead of **8**. A white solid was obtained (3.15 g, 68%). Full characterization of this molecule has been reported previously.[96,97] Raman (neat powder): $\tilde{\nu}$ 3056, 2940, 2250, 1605, 1004 cm^{-1}.

Synthesis of 1,6-Bis(dipentafluorophenylamino)-2,4-hexadiyne (3). Diyne **3** was prepared similarly to **2** by using **10** (0.70 g, 1.8 mmol) instead of **8**. A white solid was obtained (0.5 g, 72%). Mp 144.2 °C. ^{1}H NMR (200.1 MHz, $CDCl_3$): δ 4.45 (s, 4H; H3). ^{19}F NMR (235.4 MHz, $CDCl_3$): δ −162.2 (m, 8F; F6), −157.8 (t, $^3J_{FF}$ = 21.7 Hz, 4F; F7), −148.0 (m, 8F; F5). ^{13}C NMR (50.3 MHz, $CDCl_3$): δ 45.4 (C3), 70.1 (C1), 73.6 (C2), 120.7 (m; C4), 138.4 (dm, $^1J_{CF}$ = 252 Hz; C7), 140.0 (dm, $^1J_{CF}$ = 254 Hz; C6), 144.7 (dm, $^1J_{CF}$ = 249 Hz; C5). Raman (neat powder): $\tilde{\nu}$ 2269, 1658 cm^{-1}. FAB+ MS (NOBA) *m*/*z* (%): 772 (19) $[M]^+$, 424 (15) $[M-N(C_6F_5)_2]^+$. Elemental anal. Calcd (%) for $C_{30}H_4F_{20}N_2$ (772.33): C, 46.65; H, 0.52; N, 3.63. Found: C, 45.85; H, 0.78; N, 3.69.

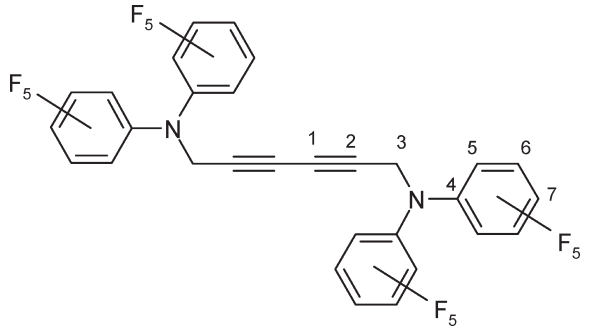

Synthesis of 1,12-Bis(diphenylamino)-5,7-dodecadiyne (5). Diyne **5** was prepared similarly to **4** by using **11** (2.0 g, 8.0 mmol) instead of **7** and DME instead of methanol. The crude product was first chromatographed on alumina with use of a 90:10 v/v mixture of *n*-pentane and dichloromethane as eluent, then it was recrystallized from acetone. A white solid was obtained (1.24 g, 62%). Mp 67.5 °C. ^{1}H NMR (200.1 MHz, $CDCl_3$): δ 1.62 (m, 4H; H4), 1.81 (m, 4H; H5), 2.31 (t, $^3J_{HH}$ = 6.7 Hz, 4H; H3), 3.75 (three peaks, 4H; H6), 6.94−7.04 (m, 12H; H8 and H10), 7.26−7.34 (m, 8H; H9). ^{13}C NMR (50.3 MHz, $CDCl_3$): δ 19.5 (C3), 26.3 (C4), 27.3 (C5), 52.1 (C6), 66.1 (C1), 77.6 (C2), 121.4 (C8), 121.6 (C10), 129.7 (C9), 148.4 (C7). Raman (neat powder): $\tilde{\nu}$ 3064, 2907, 2252, 1602, 1253, 994 cm^{-1}. FAB+ MS (NOBA) *m*/*z* (%): 497 (52) $[M+H]^+$, 328 (10) $[M-N(C_6H_5)_2]^+$. Elemental anal. Calcd (%) for $C_{36}H_{36}N_2$ (496.68): C, 87.05; H, 7.31; N, 5.64. Found: C, 87.48; H, 6.63; N, 5.46.

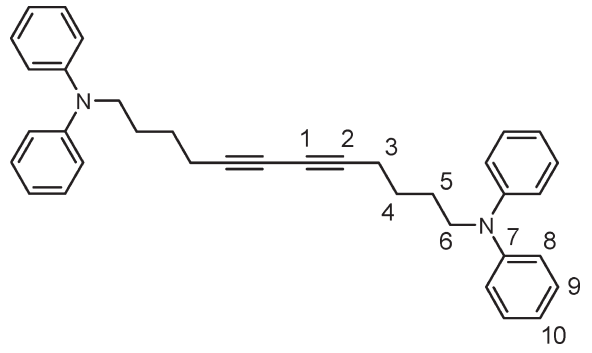

Synthesis of 1,10-Bis(diphenylamino)-4,6-decadiyne (6). Diyne **6** was prepared similarly to **2** by using **12** (5.0 g, 21.2 mmol) instead of **8**. The precipitate that formed during the reaction was collected, washed with *n*-pentane, and dissolved in dichloromethane. The dichloromethane solution was washed several times with

(96) D'hooghe, M.; Van Brabandt, W.; De Kimpe, N. *J. Org. Chem.* **2004**, *69*, 2703–2710.
(97) Sharifi, A.; Mirzaei, M.; Naimi-Jamal, M. R. *J. Chem. Res. Synopsis* **2002**, 628–630.

deionized water, dried over magnesium sulfate, and the solvent was evaporated off. A white solid was obtained (3.55 g, 71%). Mp 85.5 °C. ^{1}H NMR (200.1 MHz, $CDCl_3$): δ 1.92 (five peaks, 4H; H4), 2.38 (t, $^3J_{HH}$ = 6.9 Hz, 4H; H3), 3.85 (three peaks, 4H; H5), 6.94−7.05 (m, 12H; H7 and H9), 7.25−7.35 (m, 8H; H8). ^{13}C NMR (50.3 MHz, $CDCl_3$): δ 16.4 (C3), 26.6 (C4), 51.4 (C5), 69.3 (C1), 84.1 (C2), 121.5 (C7), 121.8 (C9), 129.7 (C8), 148.4 (C6). Raman (neat powder): $\tilde{\nu}$ 2256, 1604, 1592, 1573 (shoulder) cm^{-1}. FAB+ MS (NOBA) m/z (%): 468 (52) $[M]^+$. Elemental anal. Calcd (%) for $C_{34}H_{32}N_2$ (468.63): C, 87.14; H, 6.88; N, 5.98. Found: C, 86.45; H, 7.22; N, 5.86.

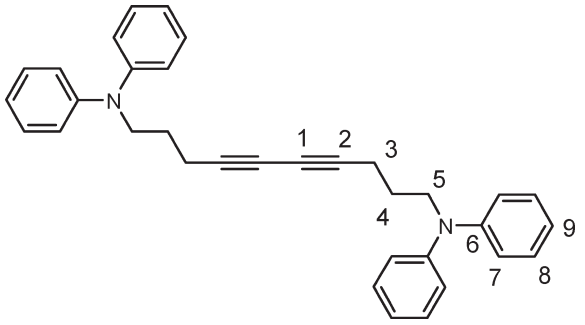

Crystal Growth. Crystals of **6** were grown from acetone at 4 °C in the dark. Depending on the concentration of the mother liquor, the dimensions and habits of the crystals can change significantly: crystals with dimensions of approximately 5 × 1 × 0.3 mm^3 were obtained when concentrated solutions were used (in this case the nucleation rate is high), whereas crystals with a length of several millimeters in each direction were obtained when dilute solutions were employed.

Thermal Polymerization. A single crystal (thickness = 310 μm) of monomer **6** was kept at room temperature (22 °C) for 160 h, then heated isothermally in an oven at 45 °C for the same amount of time, then at 70 °C. During polymerization, the absorption spectrum of the crystal was recorded periodically on a Cary 5000 spectrometer. The polymer content was measured by making use of the extinction coefficient parallel to the chains in the crystalline state, $\alpha_{//} = (7.3 \pm 1.1) \times 10^5$ cm^{-1}, determined in this work.

UV Polymerization. A crystal of diacetylene **6** (thickness = 450 μm) was cut in two pieces. Both pieces were placed in a Cary 5000 spectrometer and subjected to UV irradiation. The first fragment was irradiated at 275 nm with a power density of 375 nW/cm^2, the second fragment at 340 nm with a power density of 100 nW/cm^2.

γ-Ray Polymerization. γ-Ray polymerization experiments were carried out at the Research Section of the Curie Institute in Paris (France) with use of a ^{137}Cs γ-ray source. The irradiation equipment used was IBL 637 (CIS BIO International) n° 95−22. The dose rate was 45 Gy/min.

Several batches of crystals of **6** were placed in glass tubes and subjected to γ-ray irradiation. The transparent monomer crystals turned yellow at low doses (see Table 3), and deep orange or red at the highest doses. In the range of γ-ray doses under consideration, from 0.4 to 25 MRad, the amount of poly-**6** that was produced scaled linearly with the irradiation dose. The γ-ray polymerization rate, close to 0.75 wt % per MRad, was determined by dissolving weighted amounts of crystals irradiated with known doses of γ-rays and making use of the extinction coefficient measured in solution.

Pure poly-**6** was obtained by washing irradiated crystals with acetone (to dissolve the monomer) and collecting the insoluble solid by filtration. The red material thus isolated was washed several times with acetone to remove any remaining monomer. By doing so, tens of milligrams of pure polymer were obtained.

Molecular Weight Measurements. The number (M_n) and mass average (M_w) molecular weights of poly-**6** chains contained in single crystals of **6** exposed to γ-rays were measured by size exclusion chromatography (SEC) at the Laboratoire de Chimie des Polymères, UMR 7610 CNRS - Université Pierre et Marie Curie, Paris, France. The analytical setup was made of a Viscotek VE 7510 GPC degasser, a Viscotek VE 5200 GPC autosampler, a Waters 515 HPLC pump, three Polymer Laboratories PL-Mixed columns placed in a thermostatted oven at 40 °C, a Viscotek VE 3580 differential refractometer, and a Waters 484 UV−visible detector. The eluent was distilled THF. A 3 mg mL^{-1} THF solution of poly-**6** was filtered through a 0.45 μm membrane prior to injection. Calibration was performed using low polydispersity index polystyrene standards. It is noteworthy that, for poly-4BCMU in THF, use of polystyrene standards overestimates the masses by a factor of about 2.[98] A similar observation was made for another conjugated polymer, poly(3-hexylthiophene).[99] Assuming that this correction is also valid for poly-**6**, the experimental results, $M_n \approx$ 300 000 Da and $M_w \approx$ 870 000 Da, should be corrected to $M_n \approx$ 150 000 Da and $M_w \approx$ 435 000 Da. But the influence of the side group structure on the correction factor has not been studied, so we believe it is more appropriate to give a range for M_n, 150 000−300 000 Da.

X-ray Diffraction. Intensity measurements for compounds **1**−**5** were carried out at the joint X-ray scattering facility of the Institut Charles Gerhardt and the Institut Européen des Membranes, Université Montpellier II, France, with use of an Oxford Diffraction Xcalibur-1 CCD diffractometer. The data collection temperature was 173 K and the crystal-to-detector distance 50 mm; other data collection parameters were nearly identical in all five experiments. A total of 678 exposures were taken using ω-scans with oscillations of 1°. The counting time per frame varied from 30 to 40 s. The data were corrected for possible intensity decay and absorption using the empirical AbsPack procedure.[100] All five structures were solved by ab initio charge-flipping using the SUPERFLIP[101] computer program and refined by least-squares methods on F using CRYSTALS.[102] One crystal (**4**) turned out to be a poor scatterer. Consequently, for this crystal, atomic displacement parameters were refined only isotropically in order to keep the reflection-to-parameter ratio reasonable. Hydrogen atoms were in general located in difference Fourier maps. Their geometries were next regularized via refinement with soft restraints on bond lengths and angles and soft restraints on U_{iso}(H) (in the range 1.2−1.5 times U_{eq} of the parent atom). Lastly, their positions were refined with riding constraints. Final R values and relevant crystallographic data are given in Table 1.[48]

Single-crystal X-ray diffraction analysis of **6** was performed at the X-ray diffraction center of the Laboratoire de Chimie de Coordination in Toulouse, France. Data were collected at 180 K on a Bruker Kappa Apex II diffractometer equipped with an Oxford Cryosystems cryostream cooler device. The final unit cell parameters (Table 1) were refined from 8528 reflections. The structure was solved by direct methods using SIR92,[103] and the

(98) Rawiso, M.; Mathevet, F.; Schott, M. Unpublished results.
(99) Holdcroft, S. *J. Polym. Sci., Part B: Polym. Phys.* **1991**, *29*, 1585–1588.
(100) CrysAlis^{Pro}, Oxford Diffraction Ltd.: Oxford, U.K., 2006.
(101) Palatinus, L.; Chapuis, G. *J. Appl. Crystallogr.* **2007**, *40*, 786–790.
(102) Betteridge, P. W.; Carruthers, J. R.; Cooper, R. I.; Prout, K.; Watkin, D. J. *J. Appl. Crystallogr.* **2003**, *36*, 1487.
(103) Altomare, A.; Cascarano, G.; Giacovazzo, C.; Guagliardi, A. *J. Appl. Crystallogr.* **1993**, *26*, 343–350.

SHELXL97 program[104] was used for full-matrix least-squares refinement against F_o^2 using all reflections; both programs are part of the 1.63 version of the WinGX suite.[105] Atomic scattering factors were taken from a standard source.[106] All non-hydrogen atoms were refined anisotropically. Hydrogen atoms were positioned geometrically and refined using the riding model.[48]

Structural drawings (Figures 1−6) were prepared with use of the three-dimensional visualization system for electronic and structural analysis VESTA.[107]

Computational Details. 0 K periodic electronic structure calculations were performed using density functional theory (DFT) within the PBE[108] generalized gradient approximation (GGA), and using projector augmented-wave (PAW) pseudopotentials[109,110] as implemented in the VASP code.[111,112] The choice of the PBE-GGA functional allows to compute large systems with good accuracy and has a limited computer cost.[113] A Γ-centered $4 \times 1 \times 1$ *k*-point mesh with a high *k*-point density in the direction of the conjugated polymer chain was used. A coarser mesh in that direction induces significant modifications of both monomer and polymer structures.[114] Larger *k*-point samplings are not needed in directions perpendicular to the chain as no dispersion of the electronic band structure is observed.

6 and poly-**6** were computed using a 550 eV cutoff with, in each case, optimization of the atomic positions and, when needed, optimization of the unit cell parameters. For all systems, the residual forces on the atoms were lower than 0.01 eV $Å^{-1}$. The vibrational modes for the whole unit cells were obtained by discrete calculation of the dynamical matrix followed by a diagonalization procedure to determine the eigenvalues and eigenvectors. After that, the eigenvector can be projected on the localized C=C and C≡C stretch of the polymer backbone for identification. The optical absorption spectrum of poly-**6** was computed from an estimated dynamic dielectric constant using CASTEP.[115] A scissor operator of 0.65 eV was used in the calculations to correct for underestimation of the gap by DFT. Only band-to-band, not excitonic, transitions are modeled.

Acknowledgment. The Agence Nationale de la Recherche, France, is gratefully acknowledged for financial support of this work (Grant ANR-06-NANO-013). We are indebted to Prof. Daniel Louvard, Head of the Research Department of the Curie Institute (Paris, France), for allowing us to use the IBL 637 for irradiation of the diacetylene compounds, and to Ms. Charlotte Bourgeois from INSP for carrying out some of the γ-ray irradiation experiments described herein. We warmly thank Dr. J.-F. Morhange from INSP for his participation in the Raman studies, Ms. Ibtissam Tahar-Djebbar from the Laboratoire de Chimie des Polymères, UMR 7610 CNRS - Université Pierre et Marie Curie (Paris, France) for the SEC molecular weight determinations, and Dr. Laure Vendier (Laboratoire de Chimie de Coordination, UPR 8241, Toulouse, France) for solving the X-ray crystal structure of compound **6**. We are also grateful to the French computational resource centers IDRIS and CINES for support under contracts 071750 and x20090911750.

Supporting Information Available: Experimental details for the syntheses of alkynes **7**−**14**, full crystallographic data for the optimized structures (CIF format), and absolute energies (Table S1) . This material is available free of charge via the Internet at http://pubs.acs.org.

(104) Sheldrick, G. M. *SHELX97* [*Includes SHELXS97, SHELXL97, CIFTAB*] − *Programs for Crystal Structure Analysis* (*Release 97*−*2*); Institüt für Anorganische Chemie der Universität: Göttingen, Germany, 1998.
(105) Farrugia, L. J. *J. Appl. Crystallogr.* **1999**, *32*, 837–838.
(106) Cromer, D. T.; Waber, J. T. *International Tables for X-Ray Crystallography*; The Kynoch Press: Birmingham, U.K., 1974; Vol. *IV*.
(107) Momma, K.; Izumi, F. *J. Appl. Crystallogr.* **2008**, *41*, 653–658.
(108) Perdew, J. P.; Burke, K.; Ernzerhof, M. *Phys. Rev. Lett.* **1996**, *77*, 3865–3868.
(109) Blöchl, P. E. *Phys. Rev. B* **1994**, *50*, 17953–17979.
(110) Kresse, G.; Joubert, D. *Phys. Rev. B* **1999**, *59*, 1758–1775.
(111) Kresse, G.; Hafner, J. *Phys. Rev. B* **1994**, *49*, 14251–14269.
(112) Kresse, G.; Furthmüller, J. *Comput. Mater. Sci.* **1996**, *6*, 15–50.
(113) Paier, J.; Marsman, M.; Kresse, G. *J. Chem. Phys.* **2007**, *127*, 024103−1–024103−10.
(114) Katagiri, H.; Shimoi, Y.; Abe, S. *Chem. Phys.* **2004**, *306*, 191–200.
(115) Segall, M. D.; Lindan, P. J. D.; Probert, M. J.; Pickard, C. J.; Hasnip, P. J.; Clark, S. J.; Payne, M. C. *J. Phys.: Condens. Matter* **2002**, *14*, 2717–2744.